

1 **Authors' responses to reviews for hess-2014-444**

2 **Groundwater surface mapping informs sources of**
3 **catchment baseflow**

4
5 **J. F. Costelloe¹, T. J. Peterson¹, K. Halbert², A. W. Western¹ and J. J.**
6 **McDonnell^{3,4}**

7 [1]{Department of Infrastructure Engineering, University of Melbourne, Australia}

8 [2]{Ecole Centrale de Nantes, Nantes, France}

9 [3]{Global Institute For Water Security, University of Saskatchewan, Saskatoon, Canada}

10 [4] {School of Geosciences, University of Aberdeen, Aberdeen Scotland}

11 Correspondence to: J. F. Costelloe (jcost@unimelb.edu.au)

12
13 We thank Anonymous Referees #1 and #2 and Professor Ian Cartwright for their considered
14 and insightful reviews of our paper. Their helpful comments and suggestions have been
15 addressed below with responses to each individual comment. The page number and line
16 number of changes made in the revised manuscript are provided for each comment.

17
18 **Anonymous Referee #1**

19 **General comment 1**

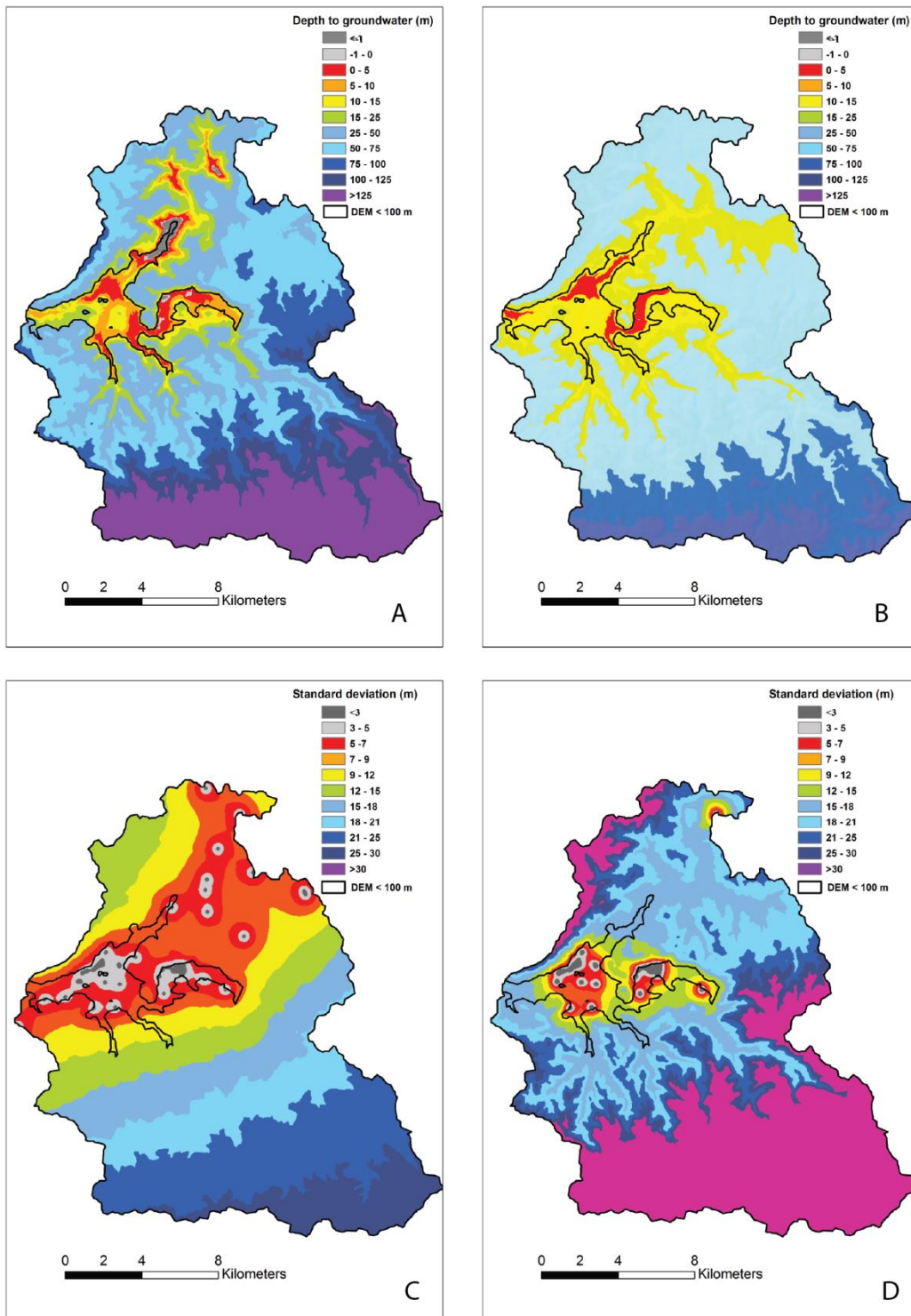
20 The bore density in the catchment (98 bores per 311 km²) seems remarkably high and is
21 primarily due to the catchment having been investigated for water supply and damming
22 purposes. This is not typical for most catchments. I wonder how the findings would fair if a
23 lower density of groundwater measures were available. Say 50% of the current density? There
24 is, of course, a break point when the geostatistics cannot really be applied anymore. Still, I
25 wonder how much value there is in the groundwater observations when fewer observations in
26 space are available. This could easily be checked by some random removal of data from the
27 entire set and then kriging the remainder. What error is introduced? Cycling through

1 realizations of the random removal in a Monte Carlo sense and systematically considering
2 10%, 20%, etc. removal would really give insights to stability and robustness of the approach.
3 It would also shine light on true added value of considering groundwater maps. This would
4 also help the study find resonance with those working in not-so-heavily instrumented sites
5 (which would likely be prevalent in most parts of the world).

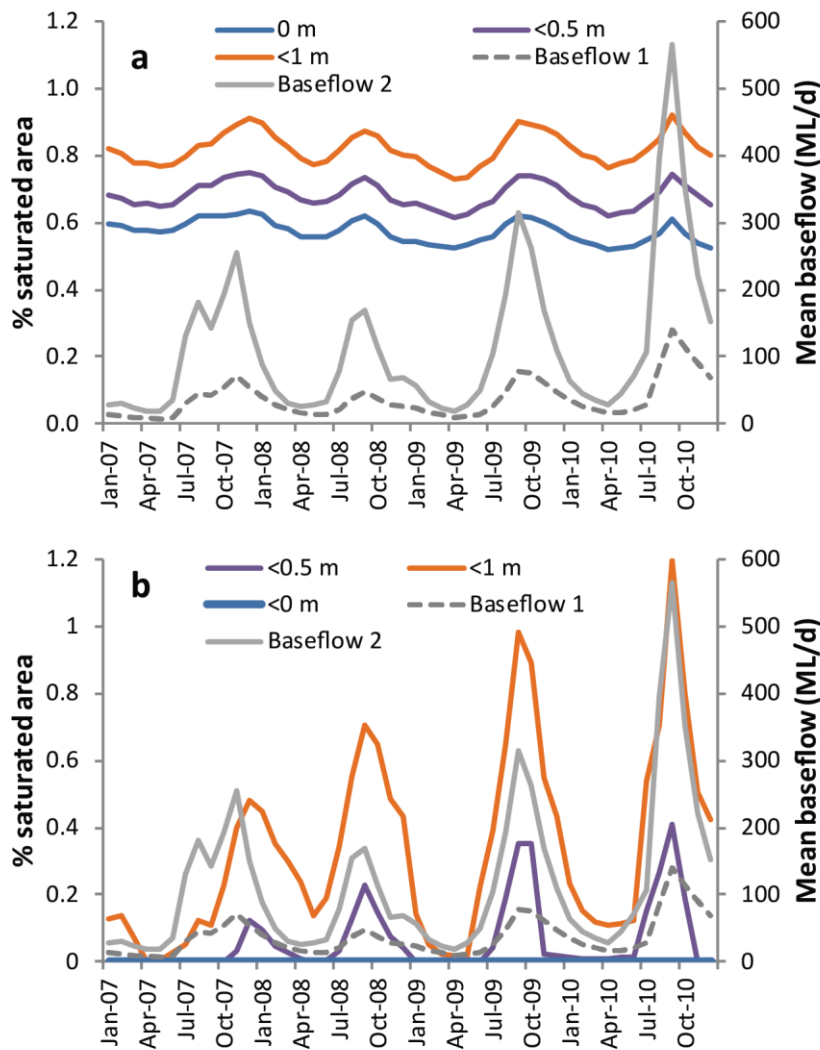
6 *Authors' response*

7 We agree that the study catchment has a unusually high density of groundwater monitoring
8 bores due to previous hydrological resource studies (note that there were actually 88 bores
9 with sufficient data for the mapping, not 98). It is for this reason that the Gellibrand
10 catchment was chosen as a case study for investigating the value of groundwater surface
11 mapping in estimating stream baseflow. It is common practice in hydrological research to
12 investigate novel techniques in highly instrumented research catchments (often of very small
13 size) for a proof of concept approach. We have taken a similar approach, albeit in a relatively
14 large catchment. As the purpose of this paper is to investigate a proof of concept, there is
15 insufficient space to conduct a rigorous Monte Carlo type analysis of the uncertainty
16 generated by the number of bores used in the groundwater mapping and such an analysis may
17 be difficult to generalise due to the uneven distribution of bores in the catchment (discussed
18 further in the text). However, as an initial analysis we have reduced the number of bores by
19 62% (significantly greater than the 50% suggested by Referee #1). This analysis generated
20 groundwater surfaces using only 33 bores within the catchment that have been screened at
21 shallow levels (<40 m). This analysis addresses both the concern of Referee #1 and also that
22 of Professor Cartwright in regards to separating deeper bores screened within the Eastern
23 View Formation. The additional analysis has been added to Section 3.4 and Figs. 5-7. Fig. 5
24 shows an example of groundwater surfaces from the two datasets. Figs. 6 and 7 show the use
25 of the two sets of data in the analysis of changes in saturated ground surface (Fig. 6) and
26 changes in saturated volume (Fig. 7) between months. The use of the two datasets in terms of
27 uncertainty analysis is discussed in Section 4.2.

28



1
 2 Figure 5. Depth to groundwater maps (A – ‘potentiometric surface’ (all bores), B – ‘water
 3 table’ (shallow bores)) and kriging standard deviation (C – potentiometric surface, D – water
 4 table) for 1st September 2009. Areas of shallow or intersecting (artesian) groundwater are
 5 restricted to the Gellibrand River (centre) and Love Creek (north) valley floors.

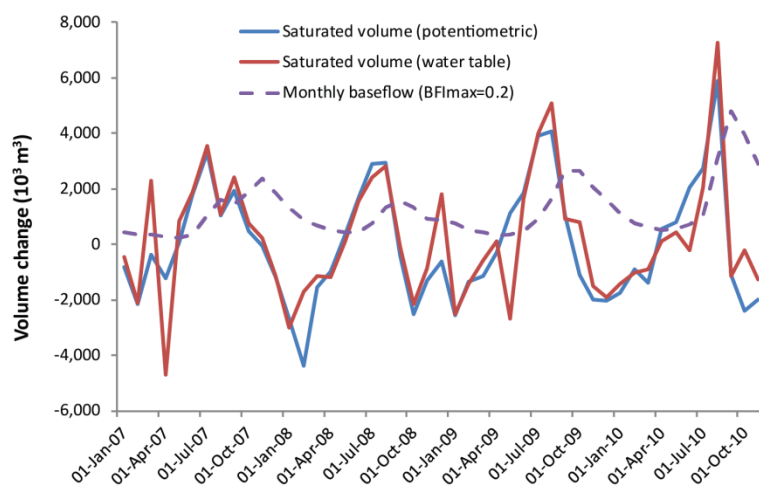


1

2 Figure 6. Percentage saturated area (intersection of groundwater surface with land surface)
 3 variations over time for the potentiometric (all bores) dataset (a) and the water table (33
 4 bores) dataset (b) for the catchment area with elevation <100 m. The position of the water
 5 table is shown for three depths (0, 0.5, 1.0 m) to allow for uncertainties in the mapping of the
 6 depth to water table. The mean daily baseflow for each month is shown for two sets of
 7 Eckhardt filter parameter values calculated from the the Bunker Hill gauging record.
 8 Baseflow 1 uses the low BFI_{max} value ($a=0.988$, $BFI_{max}=0.20$) while Baseflow 2 uses a higher
 9 BFI_{max} value ($a=0.988$, $BFI_{max}=0.60$).

10

11



1
 2 Figure 7. Monthly variations in saturated volumes for the catchment area with elevation <100
 3 m for both the potentiometric and water table datasets and for monthly baseflow derived from
 4 Eckhardt analysis (using BFI_{max} value of 0.2).

5 Section 4.2 (Discussion), P19, L26-32, P20, L1-15.

6 “ The generation of the potentiometric surface (using 88 bores) and the water table (using 33
 7 bores) gives an indication of the sensitivity of the use of groundwater surface mapping to the
 8 amount of data available. The maps generated from the two datasets showed some
 9 differences, particularly in the minimum depths to groundwater and the increase in the
 10 standard deviation of the water table dataset (e.g. see Fig. 5). The increase in the standard
 11 deviation of each monthly groundwater surface from the use of fewer bores demonstrates the
 12 expected result that confidence in the groundwater mapping analysis will decrease with fewer
 13 data points. However, in the case of the Gellibrand catchment, the similar estimates of
 14 monthly saturated volume changes from both datasets (Fig. 8) indicated that the relative
 15 differences between monthly groundwater surfaces generated by the two datasets were small.
 16 This is probably because most monitoring bores in both datasets were located in the valley
 17 floors and so confidence in the interpolated water table surfaces was highest in these areas.
 18 These areas are also of most interest in investigating groundwater – river interactions. The
 19 effectiveness of groundwater mapping as a water resource assessment tool will depend on the
 20 number of monitoring bores within a catchment but the question of how many monitoring
 21 bores are required will be highly dependent on the catchment size and spatial distribution of
 22 bores. In this study area, monitoring bores were commonly located in clusters and transects of
 23 limited length and these locations were likely determined by ease of access for drilling and
 24 the specific aims of past investigations rather than to optimise the spatial distribution of

1 groundwater observations for catchment wide water table mapping. As a result, the
2 uncertainty of groundwater surface maps would be very catchment specific and difficult to
3 generalise to other locations.”

4

5 **General comment 2**

6 The mass balance separations (Table 1) are very useful. I think these would be more useful if
7 some level of uncertainty was included in the analysis. There must be some way to show
8 uncertainty bounds in these estimates? Either by considering spatial variations across the
9 various end members and/or temporal variations in the stream samples themselves. This will
10 help demonstrate how robust the estimations are that separate between the two “unknown”
11 flows in the system. Can you make statements about differences between these two flows
12 given the uncertainty in the separation estimates?

13 *Authors' response*

14 We acknowledge that the inclusion of uncertainty analysis for the mass balance estimates is
15 required. The two end-members with the greatest range in their chemical compositions are the
16 groundwater and ungauged tributary streamflow (see Supplement A). As suggested by
17 Referee #1 and Professor Cartwright, we have investigated how this uncertainty affects the
18 mass balance estimates. This has been done by varying the groundwater ionic compositions by
19 one standard deviation, as this end-member generally has the largest variance in composition.
20 The range of valid groundwater and ungauged tributary discharges resulting from this
21 uncertainty analysis is included in Table 1. These additional analyses are explained in the
22 Methods and Results.

23 Section 2.4 (Methods), P10, L8-11.

24 “To explore the uncertainty in the mass balance estimates, the composition of the
25 groundwater end-member was varied by \pm one standard deviation, as this end-member had the
26 largest standard deviation for two of the ions (Cl, Na, see Supplement A) used in the
27 calculations.”

28

29

1 Table 1. Estimates of groundwater discharge (Q_{gw}) and ungauged tributary discharge (Q_{ut})
 2 using mass balance analysis and mean measured compositions of groundwater and ungauged
 3 tributary flow. The values within the brackets are the range of valid discharges generated by
 4 varying the groundwater composition by one standard deviation for each ion used in the
 5 analysis. Q_{res} is the residual discharge after accounting for the gauged discharges within the
 6 study catchment and the following value in brackets is the ratio of Q_{res} to the total streamflow
 7 measured at Bunker Hill gauging station.

Date	Q_{gw} (MLd ⁻¹)	Q_{ut} (MLd ⁻¹)	Q_{res} (MLd ⁻¹)	Tracer	Method
21/1/13	14.0 (4.0-14.0)	2.8 (2.8-12.8)	16.8 (0.45)	Cl-Ca	Two end-member
21/1/13	12.0 (7.0-12.0)	4.8 (4.8-9.8)	16.8 (0.45)	Cl-Mg	Two end-member
21/1/13	14.8 (1.3-14.8)	2.0 (2.0-15.5)	16.8 (0.45)	Ca-Mg	Two end-member
21/1/13	- (4.4-7.6)	- (9.2-12.4)	16.8 (0.45)	Na-Mg	Two end-member
21/1/13	- (10.3)	- (6.5)	16.8 (0.45)	Na-Ca	Two end-member
21/1/13 – 28/1/13	13.7 (5.3-13.7)	1.8 (1.8-10.2)	15.5 (0.45)	Cl	One end-member series
21/1/13 – 28/1/13	7.1 (3.8-12.6)	8.4 (2.9-11.7)	15.5 (0.45)	Na	One end-member series
21/1/13 – 28/1/13	13.7 (8.9-13.7)	1.8 (1.8-6.6)	15.5 (0.45)	Ca	One end-member series
21/1/13 – 28/1/13	13.7 (7.7-13.7)	1.8 (1.8-7.9)	15.5 (0.45)	Mg	One end-member series
21/1/13 – 28/1/13	4.7 (3.3-8.2)	10.8 (7.3-12.2)	15.5 (0.45)	¹⁸ O	One end-member series
21/1/13 – 28/1/13	8.1 (4.6-8.1)	7.5 (7.5-10.9)	15.5 (0.45)	² H	One end-member series
7/6/13	25.2 (20.5-25.4)	59.6 (59.4-64.3)	84.8 (0.43)	Cl-Na	Two end-member
7/6/13	48.8 (35.6-53.2)	36.0 (31.6-49.2)	84.8 (0.43)	Na-Mg	Two end-member
7/6/13	38.2 (7.5-38.2)	46.6 (46.6-77.3)	84.8 (0.43)	Cl-Ca	Two end-member
7/6/13	68.9 (36.6-68.9)	15.9 (15.9-48.2)	84.8 (0.43)	Cl-Mg	Two end-member
7/6/13	9.8 (9.8-16.6)	75.0 (68.2-75.0)	84.8 (0.43)	Na-Ca	Two end-member
7/6/13 - 11/6/13	- (18.8-29.9)	- (17.1-28.2)	47.0 (0.41)	Cl	One end-member series
7/6/13 - 11/6/13	2.2 (1.2-20.5)	44.8 (26.5-45.8)	47.0 (0.41)	Na	One end-member series
20/6/13	14.7 (10.0-14.9)	31.0 (30.8-35.7)	45.7 (0.38)	Cl-Na	Two end-member
20/6/13	42.4 (3.8-42.4)	3.3 (3.3-34.3)	45.7 (0.38)	Na-Mg	Two end-member
20/6/13	- (44.5)	- (1.2)	45.7 (0.38)	Cl-Mg	Two end-member
20/6/13	- (0.2-1.0)	- (34.8-35.6)	45.7 (0.38)	Cl-Ca	Two end-member
20/6/13	- (15.3-17.9)	- (17.9-20.5)	45.7 (0.38)	Na-Ca	Two end-member
18/6/13 - 20/6/13	51.9 (31.3-51.9)	0.3 (0.3-20.9)	52.2 (0.42)	Cl	One end-member series
18/6/13 - 20/6/13	- (27.3-36.4)	- (15.8-24.9)	52.2 (0.42)	Na	One end-member series
18/6/13 - 20/6/13	- (36.9)	- (15.3)	52.2 (0.42)	Cl-Na	Two end-member series
18/6/13 - 20/6/13	- (17.3-45.2)	- (7.0-34.9)	52.2 (0.42)	Ca-Mg	Two end-member series
16/12/13	5.3 (5.3-26.6)	30.6 (9.2-30.6)	35.8 (0.30)	Na-Ca	Two end-member
16/12/13	17.1 (0.2-17.1)	18.7 (18.7-35.8)	35.8 (0.30)	Cl-Ca	Two end-member
16/12/13	- (16.2-16.6)	- (19.2-19.6)	35.8 (0.30)	Na-Cl	Two end-member
16/12/13	- (3.8-12.6)	- (23.2-32.1)	35.8 (0.30)	Na-Mg	Two end-member
16/12/13	- (18.0)	- (17.8)	35.8 (0.30)	Ca-Mg	Two end-member
16/12/13	- (2.3-33.4)	- (2.4-33.6)	35.8 (0.30)	Cl -Mg	Two end-member

8

9 Section 3.3 (Results), P12, L20-23 and P13, L5-12.

10 “ The valid range of groundwater and ungauged tributary discharges generated by varying the
 11 groundwater end-member concentration by \pm one standard deviation are shown in brackets
 12 after the values generated by the mean groundwater composition in Table 1.”

13 “ Allowing for variation within the groundwater end-member composition demonstrated the
 14 uncertainty in the range of valid flux estimates. The mass balance analyses indicated that the

1 ungauged tributary flow term was often significant (consistent with field observations) but
2 difficult to separate from the groundwater discharge term. This was likely due to the
3 similarity in signature between these two end-members. The possibility of the ungauged
4 tributary flow forming a distinctively different physical end-member to regional groundwater
5 discharge (i.e. representing a different store and flow path) is further investigated in Section
6 3.5.”

7

8 **General comment 3**

9 It is confusing when considering the saturated volume estimates from the groundwater maps
10 (around P12421L5). Was the specific yield taken as 0.3 and held constant spatially over the
11 entire region? That is a fairly strong assumption given the inherent heterogeneity in soils (and
12 subsequently specific yield) one would expect both across the catchment and into the ground.
13 I would have anticipated a much more thorough consideration of the specific yield variability
14 especially since this estimate is a cornerstone of the study. Looking at the title of the study, I
15 would have expected spatial explicit estimates of water volumes coming from the
16 groundwater maps. Instead all the variability in the water table maps is filtered through a
17 constant specific yield. A better job representing the 3D variability of specific yield and its
18 subsequent impact variability in potential groundwater contribution is required. Further, the
19 uncertainty in specific yield should be considered since they are typically difficult values to
20 estimate. Regardless, this lack of accounting for soil variability in the estimations is
21 worrisome since the differencing of the groundwater maps is the more novel aspect of the
22 study. If some variability in specific yield is not considered, then it would be recommended to
23 remove these estimates (at which point the study gets a bit thin).

24 ***Authors' response***

25 A uniform specific yield value of 0.3 was used in the analysis of monthly changes in saturated
26 volume. This value was used as an upper bound on the possible groundwater contribution to
27 streamflow as this upper bound is the most comparable to baseflow filter estimation
28 (Cartwright et al., 2014). We acknowledge that accounting for spatial heterogeneity in the
29 specific yield would refine this analysis. There are no pump test data available in the
30 catchment but Atkinson et al. (2014) used a specific yield value of 0.1 for the main aquifer,
31 the Eastern View Formation (Wangerrip Group), consistent with the porosity of this unit
32 (Love et al., 1993). Other groundwater modelling studies in this region have used a specific

1 yield of 0.1 for all the main geological units in the catchment (Heytesbury Group, Eastern
2 View Formation, Otways Group, SKM (2010)). We have investigated how varying the
3 specific yield, using a realistic range, for different units affects the estimates of saturated
4 volume change for areas within the <100m mask (Table 2). Given the paucity of specific yield
5 data for the hydrogeological units within the catchment, we consider that this broad-scale
6 uncertainty analysis is robust. We note again that we are particularly concerned with
7 identifying an upper bound on the conversion of mapped saturated volume changes to
8 possible discharge to streamflow. Therefore, we consider that the range of specific yield
9 values used in the analysis (Table 2) captures that aim and this analysis is reported in the
10 Results.

11 Section 3.4 (Results), P14, L24-33, P15, L1-21.

12 “For months in the water table dataset with declining saturated volumes (i.e. periods where
13 changes in saturated volume are dominated by discharge), we used a range of specific yield
14 values to convert the total volume change to a volume of discharged water for areas within the
15 <100m mask (Table 2). There are no pump test data for the catchment but Atkinson et al.
16 (2014) used a specific yield of 0.1 to estimate recharge for the Eastern View Formation
17 (Wangerrip Group), consistent with the effective porosity of this unit (Love et al., 1993). A
18 hydrogeological modelling study in similar units of the Otway Basin used specific yield
19 values of 0.1 for both aquifers and aquitards in their calibrated model (SKM, 2010). We use a
20 range of realistic but relatively high (Nwankwor et al., 1984) specific yield values from 0.05-
21 0.3 for the different geological units within the <100 m elevation mask for the groundwater
22 surfaces (see Fig. 1). The estimates of the ratio of monthly baseflow (from Eckhardt filter) to
23 monthly mapped volume change, shown in Table 2, are generated using the same specific
24 yield values across all geological units and also by varying the values consistent with
25 expected hydrogeological properties (i.e. specific yield of alluvium > Wangerrip Group >
26 Heytesbury Group). We consider that this range of estimates based on these specific yield
27 values provides an upper bound to the groundwater discharge, particularly since any phreatic
28 evapotranspiration flux, which would also account for some of the volume changes, is not
29 considered. For the study period of 2007-2010, only three months showed a ratio of <1
30 between the monthly baseflow time-series (generated using BFI_{max} values of 0.2 and 0.6) and
31 the corresponding monthly change in mapped water table volume (i.e. saturated volume
32 change > baseflow), using the range of specific yield values. The median ratio for both

1 baseflow time-series ranged between 2.0 and 32.2 (Table 2), with more realistic (i.e. smaller)
 2 specific yield values generating the larger median ratios (i.e. saturated volume change <<
 3 baseflow) compared to specific yield values considered to represent an upper bound. The late
 4 summer to early winter period (January to June, n=17) had median ratios 10-15% less than the
 5 late winter to early summer period (July to December, n=20) but both periods had months
 6 with very large (>10) ratios. These results indicate that the monthly baseflow fluxes are
 7 significantly larger than can be explained by groundwater discharge from the valley regions
 8 during most months of the year and requires a significant additional flux of ‘slow flow’ into
 9 the river (see also Fig. 9).”

10 Table 2. Minimum, median and 90th percentile values for ratio of monthly Eckhardt filter
 11 baseflow to ‘water table’ volume changes using a range of specific yields (S_{y1} - Wangerrip
 12 Group, S_{y2} – alluvium, S_{y3} – Heytesbury Group aquitards). Filtered baseflow time-series were
 13 calculated using a value of 0.988 and BFI_{max} values of 0.2 or 0.6. Only months with declining
 14 volume changes were used in the analysis.

S_{y1}, S_{y2}, S_{y3}	Min ratio		Median ratio		90 th perc. ratio	
	$BFI_{max} = 0.2$	0.6	0.2	0.6	0.2	0.6
0.1, 0.3, 0.05	0.41	0.89	3.23	10.81	27.3	57.3
0.1, 0.2, 0.05	0.41	0.89	3.88	12.89	28.4	61.7
0.1, 0.1, 0.05	0.41	0.89	6.77	18.06	38.0	80.2
0.15, 0.3, 0.05	0.27	0.59	2.52	8.59	15.9	33.9
0.05, 0.05, 0.05	0.82	1.78	11.9	32.21	49.8	12.5
0.1, 0.1, 0.1	0.41	0.89	5.96	16.11	24.9	60.2
0.2, 0.2, 0.2	0.21	0.45	2.98	8.05	12.4	30.1
0.3, 0.3, 0.3	0.14	0.30	1.99	5.37	8.3	20.1

15

16 **General comment 4**

17 Finally, there is a lack of quantification with regards to relating the groundwater volume
 18 estimates to the hydrograph separations. The manuscript presents results as time series
 19 comparison (Figure 10 for example). Would it be more informative to relate the various
 20 techniques to each other? How similar are the various flow estimate techniques and over what
 21 periods are they more alike and more different? Currently, there is too much qualitative
 22 analysis regarding the timing of peaks in one dataset compared to another. These qualitative
 23 statements should be firmed up with some quantification and statistics. This will really drive
 24 home the utility of the groundwater maps for constraining estimates.

1 *Authors' response*

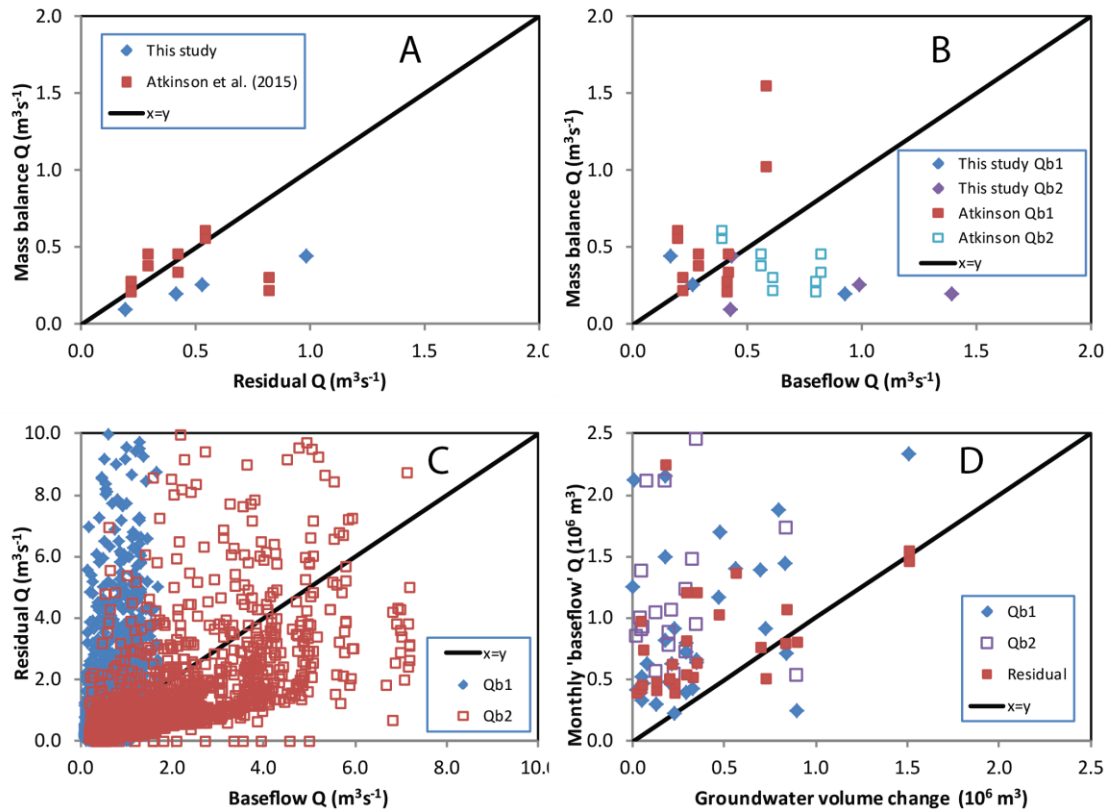
2 We have changed Figure 10 (now Figure 9) from a time series plot to a series of scatter plots
3 that better illustrate the relationships between the various estimates of baseflow and
4 groundwater discharge from our analyses. The discussion in Section 4.1 has also been
5 changed to better discuss the results presented in the revised Figure 9.

6 Section 4.1 (Discussion), P16, L17-32, P17, L1-30.

7 “Digital baseflow filters separate out the ‘slow flow’ component of streamflow. As such, they
8 provide an effective upper bound on possible groundwater discharge to streamflow
9 (Cartwright et al., 2014). This was tested by plotting scatter plots of baseflow estimates for
10 the Gellibrand River from Eckhardt digital filter analysis, residual streamflow (i.e. Bunker
11 Hill discharge less other gauged tributaries lagged by one day – Upper Gellibrand, Lardner
12 Creek, Love Creek) and tracer mass balance analyses (Fig.9 a, b, c) for the 2011-2013 period.
13 The tracer estimates include the range of estimates from Atkinson et al. (2015) for sampling
14 from known dates conducted in 2011-2012 using ^{222}Rn and Cl mass balance, plus the results
15 from this study for sampling in 2013 using major ions (shown as mid-points of the range for
16 each date shown in Table 1). None of these estimates are directly comparable as they measure
17 different components of baseflow but their comparison is informative. The digital filter time-
18 series estimates baseflow from the entire catchment upstream of Bunker Hill gauging station.
19 The Atkinson et al. (2015) estimates are for the groundwater discharge component of
20 streamflow measured over the alluvial valley reach (approximately two thirds of the Bunker
21 Hill to Upper Gellibrand reach, see Fig. 1) and use a two end-member mass balance approach
22 (tributary inflow was not considered). The tracer mass balance results from our study are for
23 the groundwater discharge component of baseflow over the Bunker Hill to Upper Gellibrand
24 reach and account for ungauged tributary inflow. For additional comparison, the residual
25 monthly discharge, monthly baseflow and the monthly saturated volume change for months
26 with decreasing volumes were plotted (Fig. 9d). The saturated volume change was calculated
27 with a realistic specific yield range (set 0.15, 0.3, 0.05 in Table 2) that produces a relatively
28 high estimate of groundwater discharge compared to estimates using other specific yield
29 values (see Table 2).

30 The tracer estimates of groundwater discharge and the residual discharge generally show a
31 consistent relationship (Fig. 9a). The Atkinson et al. (2015) estimates coincided with the
32 residual discharge, except for two outliers from one date sampled on a small rising limb, but

1 neither method separates out in-reach tributary flow from groundwater discharge. The tracer
2 estimates from this study used the residual discharge as an upper bound in their estimation
3 and so show a high correlation and a negative bias with the residual discharge. When the
4 tracer estimates are plotted against two baseflow filter estimates (Fig. 9b, using $a=0.988$,
5 $BFI_{max}=0.2$ and $a=0.988$, $BFI_{max}=0.6$) the relationships are poorly correlated and with the
6 tracer estimates both under- and over-estimating relative to the baseflow filter estimates. The
7 use of the larger BFI_{max} value (0.6), more consistent with the recommendations of Eckhardt
8 (2005), results in the tracer estimates having a more negative bias relative to the baseflow
9 filter estimates. The daily residual discharge is also compared to the baseflow filter estimates
10 over the period 2007-2013 (Fig. 9c). The use of the larger BFI_{max} value results in baseflow
11 generally higher than the residual flow (but with considerable scatter) while the lower BFI_{max}
12 value results in baseflow generally lower than the residual discharge, particularly at high
13 discharges. Finally, the mapped monthly changes in saturated groundwater volume (see Fig.
14 7) were plotted against the monthly residual discharge and baseflow filter estimates (using
15 $a=0.988$, $BFI_{max}=0.2$ and 0.6) over the 2007-2010 period (Fig. 9d). The saturated volume
16 changes were typically lower than both the residual discharge and the two baseflow
17 discharges, consistent with the the residual and baseflow measures providing an upper bound
18 to groundwater discharge within the study reach. Even the groundwater volume change is
19 more likely to represent an upper bound estimate than an unbiased estimate due to the use of a
20 relatively high specific yield range and not accounting for phreatic evapotranspiration.”



1
 2 Figure 9. Scatter plots showing various estimates of baseflow and groundwater discharge. (a)
 3 Mass balance tracer estimates (from Atkinson et al. (2015) for 2011-2012 and mid-point of
 4 range shown in Table 1 for 2013) for groundwater discharge against the residual streamflow
 5 (Bunker Hill streamflow less upstream gauged streamflow). (b) Mass balance tracer estimates
 6 against the Eckhardt filter baseflow estimates (Qb1 uses $a=0.988$ and $\text{BFI}_{\text{max}}=0.2$, Qb2 uses
 7 $a=0.988$ and $\text{BFI}_{\text{max}}=0.6$). (c) Residual discharge against Eckhardt filter baseflow timeseries
 8 for 2007-2013. (d) Saturated volume changes (using specific yield set 0.15, 0.30, 0.05 from
 9 Table 2) against residual flow and Eckhardt filter baseflow timeseries.

10 **Minor/Editorial Comments**

11 P12406L2: All “ff” where formatted strangely in my version.

12 **Authors** – Manuscript pdf file on the HESS website does not show any problems.

13 P12408L20: How does this compare to recent work by Brutsaert (2008)? Brutsaert, W.
 14 (2008), Long-term groundwater storage trends estimated from streamflow records: Climatic
 15 perspective, Water Resour. Res., 44, W02409, doi:10.1029/2007WR006518

1 **Authors** – The common use of the slowest recession curves to define one of the parameters
2 used in baseflow analysis has been explained in the Introduction and the Brutsaert (2008)
3 reference has been included.

4 Section 1 (Introduction), P3, L21-28

5 “There is typically significant variability in recession curves from a given catchment
6 suggesting a range of processes, stores and flow paths (e.g. deep and shallow groundwater
7 flowpaths, interflow, bank storage) affecting baseflow (Tallaksen, 1995; Jencso and
8 McGlynn, 2011; Chen and Wang, 2013). The regional unconfined groundwater may drive
9 only some of this response (Cartwright et al., 2014) and the baseflow derived from
10 unconfined groundwater is commonly defined by the slowest recession flows that form the
11 lower bound (e.g. the 95th percentile) of all recession curves used in the analysis (Brutsaert,
12 2008; Eckhardt, 2008).”

13 P12410L21: Well, I am guessing you mean any given date within the period of observation?

14 **Authors** – Line changed in Section 1 (Introduction, P5, L18-19) to “any given date within the
15 period of observation”.

16 P12413L14: How is having a water table 1m below the surface “nominally saturated”? I
17 appreciate the effort to consider variations in this arbitrary part of the work, but what realism
18 is retained with these values? 25cm is already quite far away from the soil surface for
19 saturation.

20 **Authors** – These depths were chosen to capture the uncertainty in the position of the
21 groundwater surface relative to the ground surface. Part of this uncertainty arises from the
22 interpolation (the error standard deviation often exceeds 1 m, Figure 5), part from the DEM
23 and also part from the fact that the DEM doesn’t capture any sub-grid scale features, such as
24 stream channels. Given this interpolation uncertainty and the possibility of groundwater
25 discharging when the water table is below the nominal DEM elevation, we feel it is necessary
26 to look at shallow water tables in addition to water tables at the surface. The text has been
27 altered to draw attention to this uncertainty.

28 Section 2.2 (Methods), P8, L6-20.

29 “ The depth to groundwater was calculated by difference from the SRTM representation of
30 the ground surface and used to measure changes in the percentage of the catchment with very
31 shallow groundwater surfaces (nominally “saturated“ within the uncertainty range of the

1 groundwater surface position) over the period of mapping. This was done for the parts of the
2 catchment with an elevation of <100 m in order to analyse changes in the saturated area
3 around the valley floor and lower slopes of the catchment where most monitoring bores were
4 located and hence confidence in the water table mapping was highest. Three threshold depths
5 to the water table (0, 0.50, 1.0 m) were used to determine changes between the seasonal
6 maximum (spring) and minimum (autumn) saturated areas. The threshold depths were not
7 calibrated but were arbitrarily chosen to capture some of the uncertainty in the groundwater
8 position (i.e. see Figure 5 for an indication of the standard deviation in the groundwater
9 surface positions) as mapped for each month. In addition, changes in total volume below the
10 mapped groundwater surface (i.e. volume containing sediments and pore spaces) between
11 months were calculated using the groundwater surface maps, again using the catchment area
12 below 100 m elevation.”

13 P12413L22: Would be good to see the equations used here to help make sense of all the
14 parameters mentioned in this section.

15 **Authors** – The Eckhardt equation has been added to the text.

16 Section 2.3 (Methods), P8, L22-27.

17 “The Eckhardt (2005) two parameter, digital recursive filter (1) was used to produce baseflow
18 time-series for the Gellibrand streamflow record at the Bunker Hill gauging station (Station
19 number 235227).

$$20 \quad b_k = \frac{(1-BFI_{max})ab_{k-1}+(1-a)BFI_{max}Q_k}{1-aBFI_{max}} \quad (1)$$

21 Where b [L^3/T] is the baseflow discharge, Q [L^3/T] is the total streamflow discharge, k [T] is
22 the time-step, and a [-] and BFI_{max} [-] are parameters requiring calibration.”

23 P12415L7: Should the ions have charges?

24 **Authors** – HESS does not require that ions are assigned charges in the text but we will accept
25 the direction of the editors on this point.

26 Figure 2: It might be the printout I am working from, but I cannot see multiple baseflow
27 separations in this figure. It would be simple to have three panels and show each separation
28 separately.

29 **Authors** – Figure 2 has been amended to show the baseflow using the mean BFI_{max} parameter
30 calculated for this study (0.2) and also using a higher BFI_{max} value (0.6) based on the work of

1 Atkinson et al. (2015) and the suggested value for perennial rivers with porous aquifers (0.8)
2 from Eckhardt (2005). The comparison with higher BFI_{max} values was suggested in the review
3 of Professor Cartwright and Fig. 2 is shown in our response to Professor Cartwright. The
4 different baseflows are shown as solid coloured lines to make the figure clearer.

5 Figure 4: Strange symbol in the word “Concentration”.

6 **Authors** – We assume that Referee #1 was referring to Figure 5 but the pdf file on the HESS
7 website does not show any problems with this figure.

8 Figure10: I cannot follow this figure. It has too many small dots and not sure what I am
9 supposed to be comparing. Would it make more sense to plot the various parameters against
10 each other rather than against time?

11 **Authors** – Figure 10 has been changed as suggested by Referee #1 and is now Figure 9 (see
12 response to general comment 4).

13

14

1 **Anonymous Referee #2**

2 **General Comments**

3 Most of my comments echo those of the previous reviewer, for example I question how well
4 this method would work with fewer data points, and I also question why the authors didn't
5 use heterogeneous subsurface properties provided they were present.

6 *Authors' response*

7 Please see responses and changes made to General Comments 1 and 2 of Referee #1

8 **Specific comments**

9 **1.** Following the usefulness of this method with reduced data points, were any of the kriging
10 parameters varied to determine the uncertainty relative to these parameters?

11 *Authors' response*

12 Further information is provided in the Methods section for how the kriging parameters used in
13 the groundwater mapping were calibrated. Essentially, the parameters were optimised to
14 reduce the variance in the mapped surfaces. The increase in the variance between the
15 potentiometric and water table sets of maps (see response to comment 1 of Referee #1) shows
16 that using fewer data points does result in increased uncertainty and changes in the Kriging
17 parameter values.

18 Section 2.2 (Methods), P7, L14-32, P8, L1-20.

19 “ In order to construct groundwater surface maps for specified dates, the periodic (generally
20 monthly) water level observations of the bore data were first modelled using the nonlinear
21 transfer-function-noise time-series modelling methodology of Peterson and Western (2014).
22 Water level estimates for the start of each month were then derived by adding the time-series
23 simulation, interpolated to the required data, to a univariate ordinary kriging estimate of the
24 timeseries model error at the required date, which ensured a zero error at dates with a water
25 level observation. groundwater surface maps were then produced for the first of each month
26 for the years 2007 to 2010 using the Kriging with external drift (KED) method (Peterson et
27 al., 2011). In applying the KED, the external drift term was the land surface elevation (Shuttle
28 Radar Terrain Model (SRTM) 30 m dataset). A model variogram was derived for the
29 component of the groundwater elevation not explained by the external drift. The KED
30 approach requires the estimation of three parameters for the residual model variogram and a

1 parameter for the maximum search radius during the mapping. Considerable effort was taken
2 to reliably calibrate the variogram parameters and set a search radius producing cross-
3 validation residuals that are approximately first-order stationary. The Kriging variance (see
4 example in Fig. 6) does provides an indicative estimate of the map reliability for the given
5 parameter set and the available water level observations. However, the density and location of
6 observations also influences the variogram parameters and the maximum search radius
7 parameter. Accounting for this parameter uncertainty in the groundwater mapping is not
8 trivial and future work is required to explore methods that account for variogram uncertainty
9 (Ortiz et al., 2002) and localised estimation of the search radius (Abedini, 2012). This
10 groundwater level component was first estimated using ordinary least squares regression and
11 then minimised by repeatedly fitting an isotropic exponential variogram, using multi-start
12 Levenberg-Marquardt optimization and re-derivation of the water level component, until a
13 stable model variogram was achieved. The depth to groundwater was calculated by difference
14 from the SRTM representation of the ground surface and used to measure changes in the
15 percentage of the catchment with very shallow groundwater surfaces (nominally “saturated“
16 within the uncertainty range of the groundwater surface position) over the period of mapping.
17 This was done for the parts of the catchment with an elevation of <100 m in order to analyse
18 changes in the saturated area around the valley floor and lower slopes of the catchment where
19 most monitoring bores were located and hence confidence in the groundwater surface
20 mapping was highest.”

21 **2.** Was any consideration given to whether the saturated areas fell in regions where surface
22 water was present (i.e. within the streambed) given that these areas would vary with stream
23 stage? For groundwater discharging to regions with little to no surface water present, was ET
24 taken into consideration?

25 ***Authors’ response***

26 The measurement of saturated areas within the catchment was used as a first-order
27 approximation of the interaction of the groundwater with the land surface. As such, we did
28 not consider how much of the saturated areas fell within the streambed and neither was ET
29 taken into consideration. Stream stage could result in local reversals in gradient between
30 groundwater and streamflow but could not be accurately determined at the scale of the 30 m
31 DEM used in the water table mapping. These aspects are addressed in Section 3.4 and 4.2.

32 Section 3.4 (Results), P14, L32-33, P15, L1-9.

1 “ We use a range of realistic but relatively high (Nwankwor et al., 1984) specific yield values
2 from 0.05-0.3 for the different geological units within the <100 m elevation mask for the
3 groundwater surfaces (see Fig. 1). The estimates of the ratio of monthly baseflow (from
4 Eckhardt filter) to monthly mapped volume change, shown in Table 2, are generated using the
5 same specific yield values across all geological units and also by varying the values consistent
6 with expected hydrogeological properties (i.e. specific yield of alluvium > Wangerrip Group
7 > Heytesbury Group). We consider that this range of estimates based on these specific yield
8 values provides an upper bound to the groundwater discharge, particularly since any phreatic
9 evapotranspiration flux, which would also account for some of the volume changes, is not
10 considered.”

11 Section 4.2 (Discussion), P19, L1-7.

12 “ Fluctuations in the water table remain a relatively coarse measure and provide only a first-
13 order estimate of possible groundwater discharge patterns. For instance, the mapping does not
14 have the resolution to identify the fine detail of channels and near-stream zones. Stage
15 variations in channels will have local effects on groundwater recharge and discharge that are
16 not captured by the groundwater mapping. Likewise, capillary fringing effects in near-stream
17 zones could lead to rapid increases in the water table with a small rise in water content in the
18 unsaturated zone (Gillham, 1984).”

19

20 **3.** Both references used on page 12407 lines 4 & 10 were found to contain significant content
21 that was improperly cited from other sources. It is recommended that the authors find the
22 original sources of the information in this work and cite those instead.

23 *Authors' response*

24 The original references have been deleted or replaced by the Bredehoeft et al. (1982)
25 reference.

26 Section 1 (Introduction), P2, L14-17.

27 “ It has been long recognised that over-extraction from aquifers may result in significant long-
28 term declines in groundwater levels resulting in decreases in baseflow in rivers (Bredehoeft et
29 al., 1982).”

30

1 4. Page 12419 Lines 7-10 are a little redundant.

2 *Authors' response*

3 These lines have been removed.

4

5

1 **Professor Ian Cartwright**

2 The main comment that I have is regarding the bores used for the water-table mapping. Being
3 familiar with the area, there are numerous groundwater bores constructed for the reasons
4 outlined in the paper. However there are two to three sets in the Gellibrand Valley. Many of
5 the bores are shallow and probably located in the near-surface alluvial aquifers that interact
6 directly with the rivers. However, there are numerous bores in the underlying confined
7 Eastern View Formation. The head levels in these two aquifers can be very different
8 (generally there are large upwards gradients between the Eastern View and the alluvials and
9 many of the deeper bores). Given the large number of bores in the area it is difficult to see
10 exactly which ones have been used for data analysis but presumably they are all in aquifers
11 that can be reasonably expected to be hydraulically connected such that a potentiometric
12 surface can be constructed. There needs to be more detail of which bores were used for this
13 analysis.

14 *Authors' response*

15 We have separated all bores from the original dataset of 88 bores in and around the catchment
16 into those with screened depths <40 m. The subset of shallow screened bores is considered to
17 represent the unconfined water table while the total dataset of bores represents more of a
18 potentiometric surface of the regional groundwater (typically in the Eastern View Formation).
19 The groundwater surfaces were mapped using both sets of bores and the results are presented
20 for both sets. The use of the smaller subset also addresses the question raised by Referee #1
21 about how sensitive the groundwater surface mapping is to a smaller set of bores being used.
22 We have also added additional supplementary material (Supplement B) detailing the bores
23 used in the study. The derivation of the two sets of groundwater surfaces are described in the
24 Methods (Section 2.2, see below) and incorporated into the analysis and results (e.g. Figs. 6,
25 7). The results and discussion have been described in our response to the first comment of
26 Referee #1

27 Section 2.2 (Methods), P7, L2-13.

28 “Eighty-eight groundwater monitoring bores in and around the boundary of the Gellibrand
29 catchment were identified and water level data were extracted from the Victorian
30 Groundwater Management System (http://www.vvg.org.au/cb_pages/gms.php). The area
31 contains a relatively large number of monitoring bores due to earlier investigations for a
32 potential damming of the Gellibrand River and also extraction of groundwater for urban water

1 supply (SKM, 2012). Groundwater surfaces were constructed from the total dataset and also
2 from a subset of 33 bores with screened depths of <40 m that only occur within the catchment
3 boundary (bore details in Supplement B). The total dataset contains bores that are screened at
4 greater depths in the Wangerrip Group (main aquifer) and these typically show higher heads
5 relative to nearby bores screened at shallower depths (typically in the Quaternary alluvium).
6 Groundwater surfaces from the total dataset represent more of a potentiometric surface while
7 the smaller dataset of shallow bores represents a water table surface.”

8

9 **Introduction**

10 **1.** I’m not sure exactly what you mean by “unconfined” – I presume that you mean an aquifer
11 that is intercepted by the stream rather than one which unconfined throughout the catchment.

12 *Authors’ response*

13 We have refined our definition of unconfined groundwater to that suggested by Professor
14 Cartwright.

15 Section 1 (Introduction), P2, L21-25.

16 “The separation of baseflow contributions from regional groundwater (i.e. where aquifers are
17 unconfined in the vicinity of streams) from other shallower sources, like interflow, bank
18 storage return and perched aquifer discharge, is technically difficult to quantify. Nevertheless,
19 this is fundamentally important for quantifying how regional groundwater extraction may
20 affect baseflow in rivers (Wittenberg, 1999).”

21

22 **2.** Given that you use both tracers and physical parameters, it is worth mentioning that these
23 techniques often yield disparate results as they classify water differently. Specifically, as
24 transient stores of water (eg bank return flows) are likely to be chemically similar to the river,
25 then a chemical mass balance will record them as event water while a digital filter will record
26 them as part of the slow flow. The last paragraph on page 12407 views baseflow from the
27 physical perspective, from a geochemical perspective baseflow is all water that looks
28 chemically different from rainfall.

29

30

1 *Authors' response*

2 In the definition of baseflow we have noted that this is from a physical perspective and also
3 identified that tracer methods can deliver different results to physically based methods.

4 Section 1 (Introduction), P2, L29-30.

5 “From a physical perspective, the baseflow component of streamflow is the sum of the slow
6 flow pathways into the river (Ward and Robinson, 2000).”

7 Section 1 (Introduction), P4, L3-10.

8 “ Tracer data are also commonly used to estimate groundwater discharge to streams (Cook et
9 al., 2003; McGlynn and McDonnell, 2003; Cartwright et al., 2011; Atkinson et al., 2015). The
10 tracer approach relies on the assumption that different contributors to streamflow have
11 distinctive and invariant chemical, isotopic or radiogenic end-member signatures that can be
12 apportioned in the streamflow mixture (McCallum et al., 2010). From a geochemical
13 perspective, mass balance estimates of baseflow using tracer data can differ from estimates
14 made by digital recursive filters as some slow flow components (e.g. bank storage) can be
15 geochemically similar to quick flow components (Cartwright et al., 2014).”

16

17 **Methodology**

18 This is generally clearly explained; however seen the comment above regarding the choice of
19 bores and the aquifers that they monitor. Also as discussed below, I think that your BFI value
20 needs more justification.

21 *Authors' response*

22 These two points have been addressed separately. The choice of bores is addressed in the
23 response to the general comment and the BFI value is addressed in the comments about
24 Results.

25

26 **Results**

27 1. The BFI used in the Eckhardt filter seems anomalously low. As explained in section 3.1,
28 values closer to 0.8 are expected for this type of catchment. Although you note this, do you
29 have an explanation? Adopting a BFI which minimises overestimates of baseflow wrt total

1 stream flow sounds logical, but are there other studies that you can point to which have done
2 this to lend some support for this methodology. I guess the related question is what the results
3 would be if a higher BFI were adopted?

4 ***Authors' response***

5 The Eckhardt filter is generally applied using the constraint that estimated baseflow \leq total
6 streamflow for each time-step. This is an arbitrary constraint and was not applied in the
7 formulation of the filter (Eckhardt, 2005). We have taken the approach of investigating use of
8 the filter without this constraint (except in the comparison of baseflow to other estimates of
9 groundwater discharge in Fig. 9) and using BFI_{max} values derived from our own analysis and
10 from the literature (Eckhardt, 2005; Atkinson et al., 2015). We have followed the
11 recommendation of Professor Cartwright to investigate the effects of higher estimates of
12 BFI_{max} in our analysis. Therefore, we have included in the analysis two additional baseflow
13 time-series using the Eckhardt (2005) recommendation of 0.8 for the BFI_{max} parameter and
14 also using the maximum BFI estimate of 0.6 identified using tracer analysis by Atkinson et al.
15 (2015) as the BFI_{max} value. The resulting differences in the estimated baseflow analysis using
16 the Eckhardt filter are shown in Figure 2 and also explained in the text in Section 2.3, 3.1, 3.4
17 (Fig. 6 – see response to comment 3 of Referee #1) and 4.1 (Fig. 9 – see response to comment
18 4 of Referee #1).

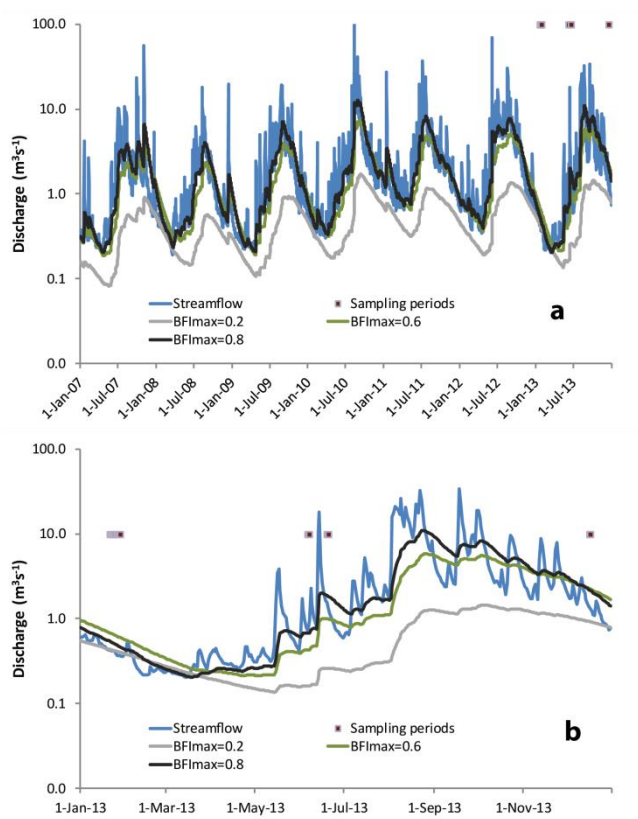
19 Section 2.3 (Methods), P9, L4-9.

20 “The BFI_{max} parameter (representing the maximum value of the baseflow index, i.e.
21 baseflow/total streamflow, that can be modelled by the filter algorithm) was chosen to
22 minimize periods of baseflow greater than observed streamflow. The filter is typically applied
23 with the condition that $b_k \leq Q_k$ (Eckhardt, 2005) but this is an arbitrary constraint and we
24 explore the resulting baseflow time-series without this condition, except where stated.”

25 Section 3.1 (Results), P10, L21-31, P11, L1-7.

26 “ The Eckhardt baseflow estimates produce patterns that follow the highly seasonal pattern
27 shown by the overall river discharge and indicated that baseflow significantly contributed to
28 overall streamflow (Fig. 2). The a parameter values declined moderately as the threshold flow
29 percentile value to define recession periods increased (30th – 0.990, 40th – 0.988, 50th –
30 0.985). The BFI_{max} parameter values that minimized periods of baseflow greater than
31 streamflow clustered around 0.2 but showed slight increases as a decreased (30th – 0.20, 40th –

1 0.20, 50th – 0.22). The resulting baseflow time-series using these parameter values were
 2 similar and the time-series using $a=0.988$ and $BFI_{max}=0.20$ is shown in Fig. 2. This method
 3 used for determining the BFI_{max} parameter produced values below the recommended range
 4 (~0.8 for perennial rivers with porous aquifers, Eckhardt, 2005) and lie closest to the
 5 recommended BFI_{max} value (0.25) for perennial rivers with hard rock aquifers. In Fig. 2 we
 6 also show baseflow time-series using $a=0.988$ and the recommended BFI_{max} value for a river
 7 such as the Gellibrand (0.80), and also using the maximum baseflow index value (0.60) found
 8 for the Gellibrand River using tracer-based analysis by Atkinson et al. (2015). Using the
 9 condition of $b_k \leq Q_k$, the filtered baseflow time-series produced mean monthly BFI estimates of
 10 0.48-0.55 ($BFI_{max}=0.20-0.22$) and 0.63-0.58 ($BFI_{max}=0.60-0.80$) during the summer-autumn
 11 period (December – May), and 0.21-0.24 ($BFI_{max}=0.20-0.22$) and 0.47-0.58 ($BFI_{max}=0.60-$
 12 0.80) during the winter-spring period (June – November)”



13
 14 Figure 2. (a) Hydrograph at Bunker Hill gauging station (235227) illustrating the seasonality
 15 of flow. Three baseflow separation hydrographs generated using different BFI_{max} parameter
 16 values (0.20, 0.60, 0.80 and $a=0.988$) for the Eckhardt filter are displayed, along with the
 17 periods of hydrochemical sampling of streamflow during 2013. (b) Hydrograph for 2013 to

1 illustrate the detail of variations in baseflow using different BFI_{max} values without the
2 constraint of $b_k \leq Q_k$.

3

4 **2.** I am not certain that the stable isotopes (section 3.3) add very much to this study. The
5 values (Fig. 4) overlap and the differences between the sampling rounds are subtle. The
6 interpretation on Page 12417 that the lower 18O values in winter possibly reflect differences
7 in source or imply a short residence time may be correct although some of the difference
8 could be related to evaporation in the warmer months increasing 18O (and this probably
9 should be mentioned if the data are retained). Without the estimate of evaporation, it is
10 difficult to use the stable isotopes for mass balance (especially given the large relative
11 variability in the groundwater).

12 *Authors' response*

13 The isotope data do not support a large influx of groundwater discharge into streamflow and
14 this is consistent with the major ion analysis and groundwater surface volume changes.
15 However, the minor differences in isotopic end-member signatures between regional
16 groundwater and tributary streamflow and possibility of evaporitic enrichment mean that the
17 isotope data do not strongly contribute to the findings of the paper. Therefore, we have
18 accepted the suggestion of Professor Cartwright and removed Figure 4 and associated isotopic
19 analysis from the paper.

20

21 **3.** Section 3.4. I am not certain that that Fig. 6 shows the difference between March and
22 September (page 12420, line 10); looking at the caption to Fig. 6, it seems to be just the
23 September data (depth to water and the SD of the kriging)? This needs clarification.

24 *Authors' response*

25 In the original Figure 6 (Fig. 5 in the revised version) the March 2009 areas of artesian
26 groundwater were shown as polygons and this was shown in the legend of the figure.
27 However, these polygons have been removed from the revised figure as the focus of the figure
28 has changed to comparing groundwater surfaces generated from the potentiometric and water
29 table datasets. In the text, to cover the point being made in the original Fig. 6, we have stated
30 that the spatial locations of areas of shallow groundwater do not vary greatly between months.

1 Section 3.4 (Results), P14, L9-17, P13.

2 “For both groundwater datasets the results are generally not consistent with changes in the
3 saturated area being the dominant driver of peak variations in baseflow, as measured by the
4 Eckhardt filter. In particular, the potentiometric dataset shows a far more consistent range in
5 seasonal peaks compared to the digital filter estimated baseflow. While the water table dataset
6 does show a similar pattern in seasonal peaks, the water table rarely reaches the land surface,
7 The saturated areas largely coincided (e.g. see Fig. 5) and were restricted to the valley floor of
8 the catchment and with little variation in the location of these areas between dates. The
9 restriction of the saturated areas to the valley floors indicates little regional groundwater
10 discharge into minor tributaries and this is analysed further in Sect. 3.5.”

11

12 **Discussion**

13 Section 4.1. The chemical mass balance would be improved by the discussion of uncertainties
14 as noted by one of the other reviewers. Possibly propagating the variability in the
15 groundwater composition through the calculations would achieve this. Additionally, the
16 impact of the assigned BFI could be considered (especially as it appears to be lower than
17 expected).

18 *Authors' response*

19 We have addressed the uncertainties in the chemical mass balance by varying the groundwater
20 end-member compositions by one standard deviation for each ion and the results are shown in
21 Table 1 and described in Section 3.3 (see response to comment 2 of Referee #1). The
22 relationship between the mass balance tracer estimates and different baseflow filter estimates
23 (particularly those generated with higher BFI_{max} values) are shown in Fig. 9 (see response to
24 comment 4 of Referee #1).

25

26 **Conclusions**

27 Some perspective regarding the impact that bore numbers and bore density has on the results
28 would be useful to researchers considering applying this to other catchments.

29 *Authors' response*

30 We have added the following text to Conclusions to provide the requested perspective.

1 Section 5 (Conclusions), P21, L2-20.

2 “ Geostatistical mapping of unconfined groundwater surfaces provides a useful, independent
3 dataset for investigating sources of fluxes contributing to baseflow estimated by traditional
4 digital filter and tracer end-member approaches. In particular, the method can provide added
5 confidence in the lower bound of baseflow estimates that best correspond to regional
6 groundwater discharge in both low and high flow periods. Specifically, the groundwater
7 surface dataset can be used to identify whether variations in discharge area (i.e. groundwater
8 intersecting the land surface) or saturated volume can explain seasonal variations in baseflow,
9 as estimated using digital filters. This dataset is particularly useful in humid, hilly catchments
10 where interflow or perched aquifer discharge is likely to be a significant process and where
11 the different ‘slow flow’ fluxes have similar low salinity chemistry that hinders end-member
12 analysis. Sufficient monitoring bore data to construct water table maps are not available in all
13 catchments and the method is likely to be restricted to catchments where groundwater
14 investigations have resulted in the existence of an adequate bore network. The adequacy of
15 the network will depend on catchment size, the spatial distribution of bores (i.e. uniform
16 versus non-uniform distribution, location relative to the drainage network) and the spatial
17 correlation of the monitored water level. However, where adequate monitoring data are
18 available, this method adds significant value to water resource management by making better
19 use of an independent, but often under-utilised, dataset that can inform groundwater
20 contributions to streamflow.”

21

22

1 **References**

- 2 Abedini, M. J., Nasser, M., and Burn, D. H.: The use of a genetic algorithm-based search
3 strategy in geostatistics: application to a set of anisotropic piezometric head data,
4 *Comput. Geosci.*, 41, 136-146, 2012.
- 5 Atkinson, A. P., Cartwright, I., Gilfedder, B. S., Cendón, D. I., Unland, N. P., and Hofmann,
6 H.: Using ¹⁴C and ³H to understand groundwater flow and recharge in an aquifer
7 window, *Hydrol. Earth Syst. Sci.*, 18, 4951–4964, 2014.
- 8 Atkinson, A. P., Cartwright, I., Gilfedder, B. S., Hofmann, H., Unland, N. P., Cendón, D. I.,
9 and Chisari, R.: A multi-tracer approach to quantifying groundwater inflows to an upland
10 river; assessing the influence of variable groundwater chemistry, *Hydrol. Process.*, 29, 1-
11 12, 10.1002/hyp.10122, 2015.
- 12 Bredehoeft, J. D., Papadopoulos, S. S., and Cooper, H. H. Jr.: Groundwater: the water budget
13 myth in scientific basis of water resource management. National Research Council
14 Geophysics Study Committee, National Academy Press, Washington, DC, pp 51–57,
15 1982.
- 16 Brutsaert, W.: Long-term groundwater storage trends estimated from streamflow records:
17 Climatic perspective, *Water Resour. Res.*, 44, W02409, doi:10.1029/2007WR006518,
18 2008.
- 19 Cartwright, I., Gilfedder, B., and Hofmann, H.: Contrasts between chemical and physical
20 estimates of baseflow help discern multiple sources of water contributing to rivers,
21 *Hydrol. Earth Syst. Sci.*, 18, 15–30, 2014.
- 22 Eckhardt, K.: How to construct recursive digital filters for baseflow separation, *Hydrol.*
23 *Process.*, 19, 507-515, 2005.
- 24 Love, A. J., Herczeg, A. L., Armstrong, D., Stadter, F., and Mazar, E.: Groundwater flow
25 regime within the Gambier Embayment of the Otway Basin, Australia: evidence from
26 hydraulics and hydrochemistry, *J. Hydrol.*, 143, 297–338, 1993.
- 27 Nwankwor, G. I., Cherry, J. A., and Gillham, R. W.: A comparative study of specific yield
28 determinations for a shallow sand aquifer, *Ground Water*, 22, 764-772, 1984.

1 Ortiz, C. J. and Deutsch, C. V.: Calculation of uncertainty in the variogram, *Math. Geol.*, 34,
2 169-18, 2002. Perrin, J., Mascré, C., Pauwels, H., Ahmed, S.: Solute recycling: An
3 emerging threat to groundwater quality in southern India, *J. Hydrol.*, 398, 144-154, 2011.
4 SKM, (2010), Glenelg Hopkins CMA groundwater model – final model development report,
5 Report to the Victorian Department of Sustainability and Environment, available at:
6 https://ensym.dse.vic.gov.au/docs/GlenelgHopkins_TransientModelReport_FINAL.pdf,
7 last access: 5 February 2015, 2010.

8 |

1 Groundwater surface mapping informs sources of 2 catchment baseflow

3
4 J. F. Costelloe¹, T. J. Peterson¹, K. Halbert², A. W. Western¹ and J. J.
5 McDonnell^{3,4}

6 [1]{Department of Infrastructure Engineering, University of Melbourne, Australia}

7 [2]{Ecole Centrale de Nantes, Nantes, France}

8 [3]{~~Global Institute For Water Security~~~~School of Environment and Sustainability~~, University
9 of Saskatchewan, Saskatoon, Canada}

10 [4] {School of Geosciences, University of Aberdeen, Aberdeen Scotland}

11 Correspondence to: J. F. Costelloe (jcost@unimelb.edu.au)

12 13 Abstract

14 Groundwater discharge is a major contributor to stream baseflow. Quantifying this flux is
15 difficult, despite its considerable importance to water resource management and evaluation of
16 the effects of groundwater extraction on streamflow. It is important to be able to differentiate
17 between contributions to streamflow from regional groundwater discharge (more susceptible
18 to groundwater extraction) compared to interflow processes (arguably less susceptible to
19 groundwater extraction). Here we explore the use of ~~unconfined~~–groundwater surface
20 mapping as an independent dataset to constrain estimates of groundwater discharge to
21 streamflow using traditional digital filter and tracer techniques. We developed groundwater
22 surfaces from ~~98-88~~ monitoring bores using Kriging with external drift and for a subset of 33
23 bores with shallow screen depths. Baseflow estimates at the catchment outlet were made
24 using the Eckhardt digital filter approach and tracer data mixing analysis using major ion ~~and~~
25 ~~stable isotope~~–signatures. Our groundwater mapping approach yielded two measures
26 (percentage area intersecting the land surface and monthly change in saturated volume) that
27 indicated that digital filter-derived baseflow significantly exceeded probable groundwater
28 discharge during ~~the high flow period of spring to early summer~~most months. Tracer analysis
29 was not able to resolve contributions from ungauged tributary flows (sourced from either

1 shallow flow paths, i.e. interflow and perched aquifer discharge, or regional groundwater
2 discharge) and regional groundwater. Groundwater mapping was able to identify ungauged
3 sub-catchments where regional groundwater discharge was too deep to contribute to tributary
4 flow and thus where shallow flow paths dominated the tributary flow. Our results suggest that
5 kriged ~~unconfined~~ groundwater surfaces provide a useful, empirical and independent dataset
6 for investigating sources of fluxes contributing to baseflow and identifying periods where
7 baseflow analysis may overestimate groundwater discharge to streamflow.

8

9 **1 Introduction**

10 Groundwater discharge is a major contributor to stream baseflow. Quantifying this flux is of
11 considerable importance to water resource management (Woessner, 2000; Sophocleous, 2002;
12 Cartwright et al., 2014). In recent decades there have been dramatic increases in the extraction
13 of groundwater for agricultural use, driven by factors such as expansion of irrigated
14 agriculture in south Asia (Llamas and Martínez-Santos, 2005; Perrin et al., 2011) and long-
15 term drought in southeastern Australia (Leblanc et al., 2012; van Dijk et al., 2013). It has been
16 long recognised that over-extraction from aquifers may result in significant long-term
17 declines in groundwater levels ~~and hence resulting in~~ decreases in baseflow ~~to in~~ rivers
18 ([Bredehoeft et al., Sophocleous, 2000 1982; 2002](#)). As a result, the switch to groundwater as a
19 source of irrigation supply has the potential to exacerbate decreases in baseflow in rivers
20 already experiencing reductions in flow from drought or instream water use. Whilst these
21 generalities of groundwater extraction and stream baseflow reduction are clear, the
22 particularities for any given catchment are complex and difficult to quantify. The separation
23 of baseflow contributions from regional ~~unconfined~~ groundwater (i.e. where aquifers are
24 unconfined in the vicinity of streams) ~~to streamflow versus from other other baseflow~~
25 ~~generation processes shallower sources, like (e.g. interflow, bank storage return, and perched~~
26 ~~aquifer discharge), is technically difficult to quantify. Nevertheless, this is but~~ fundamentally
27 important for quantifying how regional groundwater extraction may affect baseflow in rivers
28 (Wittenberg, 1999). Despite decades of work (e.g. Nathan and McMahon, 1990; Tallaksen,
29 1995; Wittenberg, 1999; Eckhardt, 2005) methods to quantify and discriminate between ‘slow
30 flow’ (itself a poorly defined term) contributions to the stream using only streamflow data are
31 approximate at best.

1 | ~~In its simplest form~~From a physical perspective, the baseflow component of streamflow is the
2 | sum of the slow flow pathways into the river (Ward and Robinson, 2000). Regional,
3 | unconfined groundwater (often termed ‘deep groundwater’) can discharge into the river via
4 | the valley floor or through more shallow, lateral flow paths, such as discharge into tributaries
5 | draining the valley slopes. ~~Interflow~~Rain event driven interflow pathways can also contribute
6 | to tributary streamflow and recent work has shown a continuum between groundwater and
7 | interflow processes (sometimes referred to as ‘shallow groundwater’ in hilly terrains) along
8 | the stream reach (Jencso et al., 2009; Jencso and McGlynn, 2011). In terms of water resource
9 | extraction (e.g. for urban supplies or irrigation on the valley floor), groundwater pumping
10 | typically targets the deep groundwater and often in alluvial valley locations where the depth
11 | to groundwater is at a minimum. Thus, it is important to be able to differentiate between
12 | contributions to streamflow from deep groundwater discharge (more susceptible to
13 | groundwater extraction) compared to shallower interflow processes (arguably less susceptible
14 | to groundwater extraction).

15 | But how can the baseflow components be identified? Digital recursive filters are the most
16 | common method of separating baseflow from streamflow but do not discriminate between the
17 | different components of baseflow and the estimate is integrated over the entire catchment area
18 | upstream of the gauging station. The technique rests on the assumption that baseflow is
19 | comprised of linear or non-linear outflow from an aquifer (e.g. Nathan and McMahon, 1990;
20 | Wittenberg, 1999; Eckhardt, 2005). All of the filter approaches require calibration of 1-3
21 | parameters based on subjective criteria (e.g. recession curve analysis, typical values, etc).
22 | Calibration of these parameters against synthetic baseflow derived from a numerical model
23 | has shown that optimal values vary considerably with catchment and climatic characteristics,
24 | many of which are not known or not possible to know *a priori* for natural catchments (Li et
25 | al., 2014).

26 | There is typically significant variability in recession curves from a given catchment
27 | suggesting a range of processes, stores and flow paths (e.g. deep and shallow groundwater
28 | flowpaths, interflow, bank storage) affecting baseflow (Tallaksen, 1995; Jencso and
29 | McGlynn, 2011; Chen and Wang, 2013). The regional unconfined groundwater may drive
30 | only some of this response (Cartwright et al., 2014) and the baseflow derived from
31 | unconfined groundwater is commonly defined by the slowest recession flows that form the
32 | lower bound (e.g. the 95th percentile) of all recession curves used in the analysis (Brutsaert,

1 | [2008; Eckhardt, 2008](#))~~additional stores and pathways can be contributing to baseflow (Jencso~~
2 | ~~and McGlynn, 2011; Chen and Wang, 2013)~~. The variable, often non-linear, baseflow
3 | response has been attributed to additional processes affecting the groundwater discharge, such
4 | as phreatic evapotranspiration (Wittenberg and Sivapalan, 1999) and recharge from soils or
5 | perched aquifers (Fenicia et al., 2006; Jencso and McGlynn, 2011). Baseflow analysis using
6 | digital recursive filters typically does not use groundwater data to constrain or test the
7 | estimates, even though baseflow should vary systematically with groundwater levels
8 | (Gonzalez et al., 2009; Meshgi et al., 2014),~~although more use is being made of tracer data~~
9 | ~~for this purpose (e.g. Cartwright et al., 2014)~~.

10 | Tracer data are also commonly used to estimate groundwater discharge to streams (Cook et
11 | al., 2003; McGlynn and McDonnell, 2003; Cartwright et al., 2011; Atkinson et al.,
12 | [2014](#)[2015](#)). ~~The tracer approach and rely relies~~ on the assumption that different contributors
13 | to streamflow have distinctive and invariant chemical, isotopic or radiogenic end-member
14 | signatures that can be apportioned in the streamflow mixture (McCallum et al., 2010). ~~From a~~
15 | ~~geochemical perspective, mass balance estimates of baseflow using tracer data can differ from~~
16 | ~~estimates made by digital recursive filters as some slow flow components (e.g. bank storage)~~
17 | ~~can be geochemically similar to quick flow components (Cartwright et al., 2014)~~. Insights
18 | have been gained ~~by in~~ heavily ~~instrumenting instrumented~~ catchments ~~to that~~ increase
19 | confidence in the identification of sources and pathways of the fluxes ~~being measured to the~~
20 | ~~stream~~—but this is usually feasible only on small experimental catchments or hillslopes
21 | (Kendall et al., 2001). In larger catchments utilised for water use, it can be difficult to separate
22 | fluxes of interest due to similarities in the tracer signatures, such as between surface flow and
23 | interflow (Kendall et al., 2001) or bank storage discharge and streamflow (McCallum et al.,
24 | 2010). This problem can be addressed by using a multiple tracer approach, so that a mix of
25 | isotopic and ionic data or conservative and radiogenic data can provide independent
26 | information on sources and pathways within a catchment (Cook et al., 2003; Cartwright et al.,
27 | 2011; Atkinson et al., [2014](#)[2015](#)). However, field studies are rarely able to identify end-
28 | members for all flow paths of interest and deep and shallow groundwater fluxes are
29 | commonly lumped together.

30 | Digital recursive filters and tracer-based analysis measure different components of baseflow
31 | and provide different bounds to the estimation of groundwater discharge. For instance, digital
32 | filter analysis provides an upper bound to groundwater discharge, integrated over the

1 upstream catchment area. Tracer analysis can provide more spatially explicit estimates of
2 groundwater discharge but can struggle with separating discharge from deep groundwater
3 flowpaths compared to shallow, lateral groundwater flowpaths. Here we argue that additional
4 datasets on groundwater dynamics are of benefit in better constraining regional groundwater
5 discharge estimates determined by these traditional methods. One overlooked measure
6 available in many catchments is groundwater level data. Intuitively, such data are directly
7 relatable to the groundwater discharge component of baseflow (Gonzalez et al., 2009; Meshgi
8 et al., 2014). More importantly, we hypothesize that groundwater observations provide
9 complementary, independent time-series of data on the dynamics of the groundwater –
10 surface water interaction.

11 The use of groundwater level data at the reach or catchment scale faces a number of
12 challenges, principally that these data are sporadically available in time and space. To
13 understand the spatial variability of groundwater throughout a catchment, various
14 geostatistical techniques have been developed to interpolate sparse groundwater level
15 observations (Desbarats et al., 2002, Boezio et al., 2006, Lyon et al. 2006). However, to date,
16 maps have been derived for only the average groundwater level at each bore, rather than
17 distributed instantaneous levels across the catchment (Desbarats et al., 2002), or at a specific
18 time using either continuous water level observations (Boezio et al., 2006, Lyon et al. 2006)
19 or basic hydrograph interpolation methods (Peterson et al., 2011) that ignore the variability
20 between observation times. Considering that groundwater observations are most often
21 collected manually and are rarely coincident across a catchment, using groundwater maps to
22 inform groundwater – surface water interaction requires maps for specific time points and
23 hence a hydrograph interpolation technique that, ideally, accounts for the variability between
24 observations. Recently, Peterson and Western (in press 2014) developed such an interpolation
25 approach for irregularly spaced observations that now allows for daily interpolated
26 observations to be generated for the estimation of groundwater surfaces for any given date
27 within the period of observation. This new method enables the generation of high frequency
28 groundwater surfaces from operational monitoring bore networks, which opens up a possible
29 new way forward for estimating groundwater contributions to baseflow.

30 Here we ~~investigate how combine~~ groundwater head data, amalgamated as water
31 table groundwater surface maps using the new Peterson and Western (in press 2014) temporal
32 interpolation ~~combined~~ with the Peterson et al. (2011) spatial interpolation approach. We

1 | ~~then use this can be used~~ as an independent and generally available ~~dataset approach~~ to
2 | constrain estimates of groundwater discharge to streamflow using traditional digital filter and
3 | tracer techniques. ~~We focus on a humid catchment in southeastern Australia where substantial~~
4 | ~~groundwater data have been collected arising from investigations of groundwater extraction~~
5 | ~~for urban water supply (SKM, 2012) and river damming. We combine 44 years of streamflow~~
6 | ~~and groundwater data observations from 98 monitoring bores across the 311 km² catchment to~~
7 | ~~investigate the utility of the groundwater data for informing sources of catchment baseflow.~~
8 | ~~We Specifically we~~ test three hypotheses:

- 9 | 1. Variations in baseflow can be explained by variations in the areas of very shallow
10 | water tables (i.e. direct discharge areas),
- 11 | 2. Variations in baseflow can be explained by changes in saturated volume between
12 | monthly water table surfaces,
- 13 | 3. Water table mapping can identify whether ungauged tributary inflow is driven by
14 | regional groundwater discharge.

15 | ~~We focus our work on a humid catchment in southeastern Australia where substantial~~
16 | ~~groundwater data have been collected arising from investigations of groundwater extraction~~
17 | ~~for urban water supply (SKM, 2012) and river damming. We combine 44 years of streamflow~~
18 | ~~and groundwater data observations from 88 monitoring bores across the 311 km² catchment to~~
19 | ~~investigate the utility of the groundwater data for informing sources of catchment baseflow.~~
20 |

21 | **2 Methods**

22 | **2.1 Study area**

23 | The Gellibrand River catchment is located in southeastern Australia in the Otway Ranges. It
24 | has a perennial, highly seasonal flow regime and a humid climate (rainfall of 1000 mm a⁻¹).
25 | The Gellibrand River is dominated by a constrained valley with much of the study reach
26 | being forested by cool temperate eucalypt rainforests, except for cleared grazing areas along
27 | the valley floor. The catchment is well gauged with gauging stations at upper Gellibrand and
28 | Bunker Hill on the Gellibrand River and gauging stations measuring flow in two of the larger
29 | tributaries (Love Creek and Lardner Creek, Fig. 1). The catchment has an area of 311 km² to a
30 | mid-catchment gauging station at Bunker Hill. Comparison of potentiometric groundwater

1 data to river levels indicates mostly gaining conditions along the Gellibrand River (SKM,
2 | 2012; Atkinson et al., [20142015](#)).

3 The southern half of the catchment, which includes the upper reaches of the Gellibrand River
4 and coincides with steep, forested terrain, is underlain by the volcanogenic sandstones,
5 siltstones and mudstones of the Cretaceous Otways Group (Fig. 1), which forms the basement
6 to the catchment. Relatively few bores occur within this unit in the Gellibrand catchment. The
7 more open, alluvial valley of the Gellibrand is underlain predominantly by fluvial sands with
8 interbedded silts and clays of the late Cretaceous Wangerrip Group and overlying Quaternary
9 alluvium. This area contains the most bores and is considered as the primary aquifer in the
10 | region (Atkinson et al., [20142015](#)). The northern half of the catchment, particularly the Love
11 Creek sub-catchment, is underlain by the marine calcareous clays of the Miocene Heytesbury
12 Group that confine the underlying aquifers in the Wangerrip Group. A number of bores occur
13 in this area but are mainly screened within the main aquifer (Eastern View Formation) of the
14 underlying Wangerrip Group.

15 **2.2 Groundwater monitoring and mapping**

16 | ~~NinetyEighty~~-eight groundwater monitoring bores in and around the boundary of the
17 Gellibrand catchment were identified and water level data were extracted from the Victorian
18 Groundwater Management System (http://www.vvg.org.au/cb_pages/gms.php). The area
19 contains a relatively large number of monitoring bores due to earlier investigations for a
20 potential damming of the Gellibrand River and also extraction of groundwater for urban water
21 | supply (SKM, 2012). [Groundwater surfaces were constructed from the total dataset and also
22 from a subset of 33 bores with screened depths of <40 m that only occur within the catchment
23 boundary \(bore details in Supplement B\). The total dataset contains bores that are screened at
24 greater depths in the Wangerrip Group \(main aquifer\) and these typically show higher heads
25 relative to nearby bores screened at shallower depths \(typically in the Quaternary alluvium\).
26 Groundwater surfaces from the total dataset represent more of a potentiometric surface while
27 the smaller dataset of shallow bores represents a water table surface.](#)

28 In order to construct ~~water-table~~[groundwater surface](#) maps for specified dates, the periodic
29 (generally monthly) water level observations of the bore data were first modelled using the
30 nonlinear transfer-function-noise time-series modelling methodology of Peterson and Western
31 | ([in-press2014](#)). Water level estimates for the start of each month were then derived by adding

1 the time-series simulation, interpolated to the required data, to a univariate ordinary kriging
2 estimate of the timeseries model error at the required date, which ensured a zero error at dates
3 with a water level observation. ~~Water-table~~Groundwater surface maps were then produced for
4 the first of each month for the years 2007 to 2010 using the Kriging with external drift (KED)
5 method (Peterson et al., 2011). In applying the ~~Kriging with external drift~~KED, the external
6 drift term was the land surface elevation (Shuttle Radar Terrain Model (SRTM) 30 m dataset).
7 A model variogram was derived for the component of the groundwater elevation not
8 explained by the external drift. The KED approach requires the estimation of three parameters
9 for the residual model variogram and a parameter for the maximum search radius during the
10 mapping. Considerable effort was taken to reliably calibrate the variogram parameters and set
11 a search radius producing cross-validation residuals that are approximately first-order
12 stationary. The Kriging variance (see example in Fig. 6) does provides an indicative estimate
13 of the map reliability for the given parameter set and the available water level observations.
14 However, the density and location of observations also influences the variogram parameters
15 and the maximum search radius parameter. Accounting for this parameter uncertainty in the
16 groundwater mapping is not trivial and future work is required to explore methods that
17 account for variogram uncertainty (Ortiz et al., 2002) and localised estimation of the search
18 radius (Abedini, 2012). This groundwater level component was first estimated using ordinary
19 least squares regression and then minimised by repeatedly fitting an isotropic exponential
20 variogram, using multi-start Levenberg-Marquardt optimization and re-derivation of the water
21 level component, until a stable model variogram was achieved. The depth to ~~water~~
22 ~~table~~groundwater was calculated by difference from the SRTM representation of the ground
23 surface and used to measure changes in the percentage of the catchment with very shallow
24 ~~water-tables~~groundwater surfaces (nominally “saturated“ within the uncertainty range of the
25 groundwater surface position) over the period of mapping. This was done for the parts of the
26 catchment with an elevation of <100 m in order to analyse changes in the saturated area
27 around the valley floor and lower slopes of the catchment where most monitoring bores were
28 located and hence confidence in the groundwater surface~~water-table~~ mapping was highest.
29 ~~Five-Three~~ threshold depths to the water table (0, ~~0.25~~, -0.50, ~~0.75~~, -1.0 m) were used to
30 determine changes between the seasonal maximum (spring) and minimum (autumn) saturated
31 areas. The threshold depths were not calibrated but were arbitrarily chosen to capture some of
32 the uncertainty in the ~~water-table~~groundwater position (i.e. see Figure 5 for an indication of
33 the standard deviation in the groundwater surface positions) as mapped for each month. In

1 | addition, changes in total volume below the [water-table mapped groundwater surface](#) (i.e.
2 | volume containing sediments and pore spaces) between months were calculated using the
3 | [water-table groundwater surface](#) maps, again using the catchment area below 100 m elevation.

4 | 2.3 Digital recursive filter analysis of baseflow

5 | The Eckhardt (2005) two parameter, digital recursive filter (1) was used to produce baseflow
6 | time-series for the Gellibrand streamflow record at the Bunker Hill gauging station (Station
7 | number 235227).

$$8 \quad b_k = \frac{(1-BFI_{max})ab_{k-1}+(1-a)BFI_{max}Q_k}{1-aBFI_{max}} \quad (1)$$

9 | [Where \$b\$ \[\$L^3/T\$ \] is the baseflow discharge, \$Q\$ \[\$L^3/T\$ \] is the total streamflow discharge, \$k\$ \[T\] is](#)
10 | [the time-step, and \$a\$ \[-\] and \$BFI_{max}\$ \[-\] are parameters requiring calibration.](#) The Eckhardt filter
11 | separates the slow flow component of the stream hydrograph based on the groundwater
12 | discharge being linearly proportional to the unconfined aquifer storage. This filter was chosen
13 | as it has a physical basis and produces results comparable with other digital recursive filters
14 | (Eckhardt, 2008). The a parameter (representing the recession constant of streamflow) was
15 | determined by the 95th percentile upper bound of the scatter plot of daily discharge (Q_k)
16 | against discharge from the next day (Q_{k+1}). These data points were extracted for recession
17 | flows of five days or longer (see Eckhardt, 2008) below a selection of percentiles of total
18 | flows (i.e. 30th, 40th, 50th). The BFI_{max} parameter (representing the maximum value of the
19 | baseflow index, i.e. baseflow/total streamflow, that can be modelled by the filter algorithm)
20 | was chosen to minimize periods of baseflow greater than observed streamflow. [The filter is](#)
21 | [typically applied with the condition that \$b_k \leq Q_k\$ \(Eckhardt, 2005\) but this is an arbitrary](#)
22 | [constraint and we explore the resulting baseflow time-series without this condition, except](#)
23 | [where stated.](#) Time-series of baseflow were then defined using the selected pairs of parameter
24 | values to represent a possible envelope of baseflow for the study catchment.

25 | 2.4 Hydrochemical sampling and analysis

26 | Water samples from streamflow were collected by automatic samplers (ISCO) at several
27 | locations in the catchment, including upstream (Upper Gellibrand gauging station and Sayers
28 | Bridge, see Fig. 1) and downstream (Bunker Hill gauging station) locations from the
29 | Gellibrand River and from major tributaries in January and June 2013. Grab samples were
30 | also collected from smaller, ungauged tributaries and from the Gellibrand River during the

1 sampling period and also in December 2013. Unconfined groundwater samples were taken
 2 from bores in the alluvial area of the Gellibrand River (some data supplied by Dr Alex
 3 Atkinson, Monash University, see Atkinson et al., [20142015](#)) after purging 2-3 well volumes
 4 of bores or until field water parameters (e.g. electrical conductivity, pH, temperature) had
 5 stabilised. Samples were filtered through a 0.45 µm membrane filter and the cation aliquots
 6 were further acidified to pH <2 using 1M HNO₃ and stored at 4°C until analysis at the
 7 Research School of Earth Science laboratory, Australian National University. Cation analyses
 8 were performed by ICP mass spectrometry (Varian Vista AX CCD Simultaneous ICP-OES)
 9 and anion analysis performed by ion chromatography (Dionex Series 4500i). Colourimetric
 10 alkalinity titrations were performed using a Hach® field titration kit. ~~Stable isotope ratios~~
 11 ~~were measured at the University of Melbourne by laser spectroscopy (Picarro cavity ringdown~~
 12 ~~spectrometer). Isotope ratios are reported to known values of a series of in-house standards~~
 13 ~~that were initially individually calibrated to International Atomic Agency Standards (IAEA)~~
 14 ~~Vienna Standard Mean Ocean Water (VSMOW) (0.0‰ δ¹⁸O, 0.0‰ δ²H), Greenland Ice~~
 15 ~~Sheet Precipitation (GISP) (-24.8‰ δ¹⁸O, -189.5‰ δD) and Standard Light Antarctic~~
 16 ~~Precipitation 2 (SLAP2) (-55.5‰ δ¹⁸O, -427.5‰ δD). Three repeat samples were run per~~
 17 ~~batch to evaluate reproducibility. The instrument precision of the Picarro is 0.3‰ for δD and~~
 18 ~~0.1‰ for δ¹⁸O.~~

19 Mass balance calculations were conducted on the streamflow samples using selected ions (Cl,
 20 Na, Ca, Mg) ~~and stable isotopes (¹⁸O, ²H) using~~ a multiple end-member model. The
 21 hydrochemical samples included upstream and downstream (gauged) locations on the
 22 Gellibrand River, major gauged tributaries and a range of smaller, ungauged tributaries. The
 23 mass balance for a gaining reach is defined by the load ([42](#)) and the discharge ([23](#)).

$$24 \quad Q_{ds}C_{ds} = Q_{us}C_{us} + Q_{gw}C_{gw} + Q_{ut}C_{ut} + Q_{gt}C_{gt} \quad (42)$$

$$25 \quad Q_{ds} = Q_{us} + Q_{gw} + Q_{ut} + Q_{gt} \quad (23)$$

26 Where Q is discharge and C is concentration and the subscripts refer to; ds – downstream
 27 Gellibrand (Bunker Hill gauging station), us – upstream Gellibrand, gw – groundwater, ut –
 28 ungauged tributaries, gt – gauged tributaries. The unknowns in the above equations are Q_{gw}
 29 and Q_{ut} and to solve require two sets of concentrations, or a single tracer with data over two or
 30 more days. This approach accounts for the contribution from the alluvial groundwater in the
 31 reach between the Upper Gellibrand and Bunker Hill gauging stations. [To explore the](#)
 32 [uncertainty in the mass balance estimates, the composition of the groundwater end-member](#)

1 [was varied by \$\pm\$ one standard deviation, as this end-member had the largest standard deviation](#)
2 [for two of the ions \(Cl, Na, see Supplement +A\) used in the calculations.](#)

3 **3 Results**

4 We first analyse the baseflow characteristics of the river using the Eckhardt (2005) baseflow
5 filter. Second, the streamflow chemical ~~and isotopic~~ patterns are presented and third, mass
6 balance analysis is used to estimate groundwater discharge and ungauged tributary discharge.
7 Finally, using the results of mapping the ~~unconfined~~ groundwater surfaces, we analyse
8 relationships between the three datasets (groundwater surfaces, baseflow filter estimates, mass
9 balance tracer estimates) and explore how the groundwater surfaces can be used to constrain
10 estimates of groundwater discharge derived from ionic mass balance and baseflow filter
11 analyses.

12 **3.1 Baseflow analysis**

13 The Eckhardt baseflow estimates produce patterns that follow the highly seasonal pattern
14 shown by the overall river discharge and indicated that baseflow significantly contributed to
15 overall streamflow (Fig. 2). The ~~α - a~~ parameter values declined moderately as the threshold
16 flow percentile value to define recession periods increased (30th – 0.990, 40th – 0.988, 50th –
17 0.985). The BFI_{max} parameter values that minimized periods of baseflow greater than
18 streamflow clustered around 0.2 but showed slight increases as ~~α - a~~ decreased (30th – 0.20, 40th
19 – 0.20, 50th – 0.22). [The resulting baseflow time-series using these parameter values were](#)
20 [similar and the time-series using \$a=0.988\$ and \$BFI_{max}=0.20\$ is shown in Fig. 2.](#) This method
21 used for determining the BFI_{max} parameter produced values below the recommended range
22 (~0.8 for perennial rivers with porous aquifers, Eckhardt, 2005) and lie closest to the
23 recommended BFI_{max} value (0.25) for perennial rivers with hard rock aquifers. [In Fig. 2 we](#)
24 [also show baseflow time-series using \$a=0.988\$ and the recommended \$BFI_{max}\$ value for a river](#)
25 [such as the Gellibrand \(0.80\), and also using the maximum baseflow index value \(0.60\) found](#)
26 [for the Gellibrand River using tracer-based analysis by Atkinson et al. \(2015\).](#) ~~The~~ [Using the](#)
27 [condition of \$b_k \leq Q_k\$, the](#) filtered baseflow time-series produced mean monthly BFI estimates of
28 0.48-0.55 [\(\$BFI_{max}=0.20-0.22\$ \) and 0.63-0.58 \(\$BFI_{max}=0.60-0.80\$ \)](#) during the summer-autumn
29 period ~~(January–December – May)~~, and 0.21-0.24 [\(\$BFI_{max}=0.20-0.22\$ \) and 0.47-0.58](#)
30 [\(\$BFI_{max}=0.60-0.80\$ \)](#) during the winter-spring period (June – November).

3.2 Streamflow chemistry and stable isotope patterns

Streamflow and groundwater samples of the Gellibrand catchment have similar Na-Cl-HCO₃ compositions (Supplement A) and are further examined using a Piper diagram (Fig. 3). The upstream, downstream and major tributary flow compositions plot closely together, with the downstream composition showing a shift towards the alluvial groundwater composition, relative to the upstream composition. However, seasonal changes in streamflow chemistry are also apparent with winter samples (June 2013) plotting closer to the groundwater composition (higher Cl, lower HCO₃) in comparison to the summer low flow samples (January and December 2013). The ungauged (minor) tributary samples show a greater spread in compositions, with only the largest of the ungauged tributaries (Charley's Creek, 47.4 km²) plotting with the gauged streamflow (Gellibrand, Love, Lardner), and others plotting in and around the alluvial groundwater compositions. The Charley's Creek subcatchment drains the southern half of the catchment underlain by the Otways Group and has a relatively similar area to the two gauged tributaries (Lardner Creek 51.8 km², Love Creek 76.6 km²). The ungauged tributaries show a greater spread in composition than the alluvial groundwater but this was dominated by relatively high Mg and SO₄ concentrations in two tributaries whilst the other tributaries were slightly depleted in Ca and K compared to the alluvial groundwater. The Love Creek samples have significantly higher ionic concentrations than all other streamflow samples in the catchment (Supplement A) but have similar ionic ratios, as shown by plotting closely to the gauged streamflow samples in Fig. 3.

~~The stable isotope data show that the winter streamflow samples (e.g. June 2013) were more depleted than summer (e.g. January 2013) samples with the early summer (December 2013) samples having intermediate values (Fig. 4). This indicates either a short residence time (i.e. streamflow samples match a seasonal shift in rainfall isotopic signal) or a shift in the mix of sources of streamflow. The mean Global Network of Isotopes in Precipitation (GNIP) Melbourne winter rainfall signature is $\delta^{18}\text{O}$ of -5.6‰ and $\delta^2\text{H}$ of -33.5‰ while the mean summer rainfall signature is $\delta^{18}\text{O}$ of -3.5‰ and $\delta^2\text{H}$ of -16.6‰ (www.naweb.iaea.org/naweb/ih/IHS_resources_gnip<http://nucleus.iaea.org/CIR/CIR/GNIP/IHS.html>). Compared to the seasonal shift in isotopic signature (Fig. 4), there was not much differentiation within individual trips between upper and lower catchment or major and minor tributaries (data not separated by criteria in Fig. 4). For the winter sampling period, all of the streamflow samples plot more closely to alluvial groundwater samples compared to the~~

1 | ~~summer samples.~~

2 The dominance of the contribution of groundwater discharge to streamflow during summer
3 low flow periods was also investigated by examining how tracer values changed during the
4 recession of flow events during the summer (January 2013) sampling period (Fig. 5). In
5 general, only the chloride data showed an approximately linear increase in concentration that
6 would be expected if the groundwater discharge flux contributed proportionally more to
7 streamflow during the short-term recession. The other major ions (e.g. Na, Ca, Mg) ~~and~~
8 ~~isotope values~~ remained relatively consistent or showed a variable pattern over time during
9 the flow recession. In addition, the streamflow composition remains distinct from the
10 groundwater composition even during the summer low flow periods (Fig. 3, 4). These patterns
11 suggest that other end-member fluxes need to be considered during the flow recession rather
12 than a simple two end-member system (i.e. upstream streamflow and groundwater discharge).

13 The compositional similarities of the ungauged streamflow samples to the alluvial
14 groundwater samples, compared to the gauged streamflow samples, raises the question
15 whether the minor ungauged tributaries represent discharged groundwater. Alternatively, the
16 ungauged streamflow may be driven by perched aquifer or similar interflow type processes. If
17 the ungauged tributary samples represent a distinct source from the regional groundwater,
18 then their chemical similarity to the groundwater samples could result in chemical mass
19 balance techniques that do not consider the contribution from ungauged tributaries,
20 overestimating the groundwater contribution to streamflow (Sect. 3.3).

21 **3.3 Mass balance analysis**

22 | Mass balances were calculated using Cl, Na, Ca, ~~and Mg,~~ ¹⁸O ~~and~~ ²H results from samples
23 collected in January, June and December 2013 (Table 1). The January 2013 period covered a
24 consistent recession period (see Fig. 54) while the June 2013 period included a flow event
25 midway through the sampling period. The December 2013 sampling covered a two day
26 'snapshot' during a recession period. The valid range of groundwater and ungauged tributary
27 discharges generated by varying the groundwater end-member concentration by ± one
28 standard deviation are shown in brackets after the values generated by the mean groundwater
29 composition in Table 1.

30 In January 2013, the selected ions showed similar downstream (i.e. Sayers Bridge to Bunker
31 Hill) percentage increases (62-82%) during the recession events and cross plots (not shown)

1 indicated that Na, Ca and Mg were showing conservative behavior relative to Cl. ~~The stable~~
2 ~~isotope data showed smaller percentage changes (1-11%) to more depleted values moving~~
3 ~~downstream.~~ The mass balance analysis (Table 1) showed that a range of the groundwater
4 discharge and ungauged tributary term values were valid generally dominated during this
5 ~~period of low flow (particularly using two end member analysis) but that the ungauged~~
6 ~~tributary discharge could also be a significant term~~, even during summer low flow conditions.
7 This was consistent with field observations that a number of the larger ungauged tributaries
8 were flowing in January 2013 and this was also the case in the June and December 2013 field
9 ~~trips. A number of combinations of end-members could not return physically realistic~~
10 ~~estimates (i.e. one discharge term being negative).~~ For the single end member, time series
11 ~~analysis, the estimates with groundwater dominating did not reach an optimal solution~~
12 ~~because of the constraint that the tributary inflow could not be negative.~~

13 In June 2013, before and after a flow event, the selected ions showed more variable
14 downstream (i.e. Upper Gellibrand to Bunker Hill) percentage increases (57-124%) ~~while the~~
15 ~~stable isotopes did not show any consistent pattern between upstream and downstream flow.~~
16 The resulting mass balance analyses again showed a range of contributions from the
17 groundwater discharge and ungauged tributary flow terms (Table 1). A number of
18 combinations of end-members could not return physically realistic estimates (i.e. one
19 discharge term being negative). ~~The single and double end member, time series analyses did~~
20 ~~not reach an optimal solution, with either the tributary inflow or groundwater discharge term~~
21 ~~being limited by the non-negative flux constraint.~~

22 Allowing for variation within the groundwater end-member composition demonstrated the
23 uncertainty in the range of valid flux estimates. The mass balance analyses indicated that the
24 ungauged tributary flow term was often significant (consistent with field observations) but
25 difficult to separate from the groundwater discharge term. This was likely due to the
26 similarity in signature between these two end-members. The possibility of the ungauged
27 tributary flow forming a distinctively different physical end-member to regional groundwater
28 discharge (i.e. representing a different store and flow path) is further investigated in Section
29 3.5. ~~There was also significant variation within each of the end-member compositions and the~~
30 ~~use of mean concentrations in the mass balance analyses is likely to contribute to the~~
31 ~~uncertainty in flux estimates.~~

3.4 Baseflow – water table dynamics

The monthly time-series of ~~water table~~groundwater surface mapping ~~from both the~~ 'potentiometric' dataset (88 bores) and the 'water table' dataset (33 bores) allows analysis of the dynamics of the relationship between baseflow and ~~water table~~groundwater fluctuations and of the spatial distribution of shallow ~~water table~~groundwater relative to the sampling of ungauged tributaries. ~~Water table~~Both sets of groundwater maps showed approximately similar patterns but with the water table surfaces being slightly deeper and with higher standard deviations (see example in Fig. 5). The maps showed that areas with ~~the water table~~groundwater ≤ 1.5 m from the ground surface were confined to the alluvial plains of the Gellibrand River and one of its major gauged tributaries, Love Creek, and these areas coincided with lower standard deviations in the water table mapping (Fig. 65). The areas of very shallow ~~water tables~~groundwater (0 m, ~~<0.25 m,~~ <0.5 m, ~~<0.75 m,~~ <1 m below the ground surface) were tabulated and plotted for both the 'potentiometric' dataset and the 'water table' dataset (Fig. 7a6) to identify areas where the groundwater could discharge to the surface or into channels within the uncertainty range of the groundwater mapping. The percentage changes in 'saturated area' (i.e. water tables within a specified depth to surface) showed different behavior between the potentiometric and water table datasets. The potentiometric dataset showed areas of artesian head along the valley floors and consistent small seasonal variations with only minor differences between years. For example, the difference between the spring (September-October) peak and autumn (April-May) trough were low in absolute terms (<0.15% of area <100m in elevation) and relative terms (9-19% variation between peaks and troughs). In contrast, the water table dataset showed groundwater heads remained below the land surface but did show much larger variations in absolute area (e.g. <1.2% of area for groundwater surfaces within 1 m of the land surface) and relative size of peaks (e.g. 80-100%) between years compared to the potentiometric dataset. ~~An example is shown in Fig. 6 of the difference in the area with the water table at the surface between March and September 2009.~~ In comparison, the ~~mean of the three~~ two baseflow time-series (using BFI_{max} parameter values of 0.2 and 0.6, see Section 3.1) showed large relative variations of ~~72-90~~95% between peaks and troughs that was similar to the peak seasonal variation shown by the water table surfaces but not to the potentiometric surfaces. The peak saturated areas typically coincided with peak estimated baseflow, except for 2007. For both groundwater datasets ~~but, unexpectedly,~~ the results are generally not consistent with ~~years with lower saturated area (e.g. 2010) have higher baseflow for a given saturated area than years with~~

1 ~~larger saturated areas. This indicates that peak changes in the saturated area are not being the~~
2 ~~dominant driver of peak variations in baseflow, as measured by the Eckhardt filter. In~~
3 ~~particular, the potentiometric dataset shows a far more consistent range in seasonal peaks~~
4 ~~compared to the digital filter estimated baseflow. While the water table dataset does show a~~
5 ~~similar pattern in seasonal peaks, the water table rarely reaches the land surface. The~~
6 saturated areas ~~largely coincided (e.g. see Fig. 5) and~~ were restricted to the valley floor of the
7 catchment ~~and with little variation in the location of these areas between dates. The restriction~~
8 ~~of the saturated areas to the valley floors, indicating indicates~~ little regional groundwater
9 discharge into minor tributaries and this is analysed further in Sect. 3.5.

10 ~~The relationship between the monthly percentage change in saturated area and the estimated~~
11 ~~monthly baseflow using the Eckhardt filter was also examined for each year (Fig. 7b). The~~
12 ~~relationship shows hysteresis with the rising limb generally being steeper and more non-linear~~
13 ~~compared to the falling limb. The peak saturated area does typically coincide with peak~~
14 ~~estimated baseflow (except for 2007) but, unexpectedly, years with lower saturated area (e.g.~~
15 ~~2010) have higher baseflow for a given saturated area than years with larger saturated areas.~~
16 ~~This indicates that peak changes in the saturated area are not the dominant driver of peak~~
17 ~~variations in baseflow, as measured by the Eckhardt filter.~~

18 The ~~comparison between~~ analysis of monthly changes in saturated volume and mean monthly
19 Eckhardt baseflow (Fig. 8) provides further evidence that the regional groundwater discharge
20 is not the major driver of the baseflow time-series. The ~~baseflow time-series show that peak~~
21 ~~annual baseflow amount steadily increased between 2008 and 2010, a pattern mirrored by the~~
22 ~~total streamflow (see Fig. 2). However, over this period the~~ saturated volume changes (at
23 elevations <100 m) ~~did not show any increasing trend~~ for both the potentiometric and water
24 ~~table datasets (Fig. 7) were similar, except for 2007 when the~~ but with the water table dataset
25 ~~showing greater variability between months-. The water table variation showed an expected~~
26 ~~seasonal pattern of peak increases in winter and peak decreases in summer. The baseflow~~
27 ~~time-series showed a lagged response with peak baseflow occurring in spring. For months in~~
28 ~~the water table dataset with declining saturated volumes~~ changes (i.e. periods where changes
29 in saturated volume are dominated by discharge), we used a range of specific yield ~~of~~
30 0.3 values to convert the total volume change to a volume of discharged water for areas within
31 the <100m mask (Table 2). There are no pump test data for the catchment but Atkinson et al.
32 (2014) used a specific yield of 0.1 to estimate recharge for the Eastern View Formation

(Wangerrip Group), consistent with the effective porosity of this unit (Love et al., 1993). A hydrogeological modelling study in similar units of the Otway Basin used specific yield values of 0.1 for both aquifers and aquitards in their calibrated model (SKM, 2010). We use a range of realistic but relatively high (Nwankwor et al., 1984) specific yield values from 0.05-0.3 for the different geological units within the <100 m elevation mask for the groundwater surfaces (see Fig. 1). The estimates of the ratio of monthly baseflow (from Eckhardt filter) to monthly mapped volume change, shown in Table 2, are generated using the same specific yield values across all geological units and also by varying the values consistent with expected hydrogeological properties (i.e. specific yield of alluvium > Wangerrip Group > Heytesbury Group). We consider that this range of estimates based on these specific yield values ~~larger specific yield values is are~~ ~~(are high (Nwankwor et al., 1984) and so likely~~ provides an upper bound to the groundwater discharge, particularly since any phreatic evapotranspiration flux, ~~which would also account for some of the volume changes,~~ is not considered. ~~For the study period of 2007-2010, only three months showed a calculated value of the ratio of <1~~ between the monthly baseflow ~~time-series (generated using BFI_{max} values of 0.2 and 0.6)~~ and the corresponding monthly change in mapped water ~~table~~ volume ~~(i.e. saturated volume change > baseflow), using the range of specific yield values.~~ The median ratio for both baseflow ~~time-series~~ ranged between 2.0 and 32.2 (Table 2), with more realistic (i.e. smaller) specific yield values generating the larger median ratios (i.e. saturated volume change << baseflow) compared to specific yield values considered to represent an upper bound, ~~with a mean of 4.4.~~ The late summer to ~~early~~ winter period (~~February–January to August~~June, n=517) had a ~~mean~~median ratios of 0.610-15% ~~less than~~ (i.e. saturated volume change greater than baseflow) while the ~~spring–late winter~~ to early summer period (~~September July to January~~December, n=1320) had a mean ratio of 7.0 (but both periods had months with very large (>10) ratios i.e. saturated volume change << baseflow). These ~~ratios–results~~ indicate that the monthly baseflow fluxes are significantly larger than can be explained by groundwater discharge ~~from the valley regions~~ during ~~the spring to early summer period~~most months of the year and requires a significant additional flux of ‘slow flow’ into the river (see also Fig. 109).

3.5 Relationship between groundwater and tributary chemistry

The relationship between regional groundwater and ungauged tributary chemistry was examined by grouping subcatchments using the depth to ~~water~~tablepotentiometric

1 | [groundwater](#) upstream of each sampling point on the ungauged tributaries. The subcatchment
2 | areas ranged from 0.4 to 47.4 km² (mean 11.0 km²) and the seasonal peak [water](#)
3 | [tablegroundwater](#) level in September 2010 was used in the analysis as it was a representative
4 | period of seasonal high [water-tablegroundwater levels](#) for the study period. The minimum
5 | monthly [water-tablegroundwater](#) depths within the subcatchments ranged between -6 (i.e.
6 | above ground surface) to 84 m below ground surface. Given the uncertainty in the minimum
7 | mapped position of the [water-tablegroundwater](#) surface (i.e. see the mapped standard
8 | deviation of the [water-tablegroundwater](#) position in Fig. 65), the subcatchments were
9 | arbitrarily divided between those with groundwater within 5 m of the land surface anywhere
10 | within the sub-catchment (i.e. where groundwater discharge [into channels](#) within the
11 | subcatchment was possible) and those with deeper groundwater (Fig. 98). There were no
12 | significant differences in the tributary compositions in subcatchments with shallow
13 | groundwater (i.e. minimum [water-tablesdepths](#) <5 m from the ground surface) or deep
14 | groundwater. These results suggest that seasonal regional groundwater [table-level](#) rises are not
15 | likely to drive seasonal increases in ungauged tributary inflow from the upper parts of the
16 | catchment. This is consistent with the chemistry of the major tributaries being similar to that
17 | of the Gellibrand River flow rather than that of the alluvial groundwater (Fig. 3). Therefore,
18 | seasonal increases in ungauged tributary inflow are more likely to be driven by interflow or
19 | perched aquifer processes, rather than variations in the regional [unconfined](#)-groundwater. The
20 | baseflow filter estimates show large increases in the 'slow flow' component of streamflow
21 | during winter-spring periods that were not consistent with probable groundwater discharge
22 | (Fig. 87). The mass balance calculations indicate that small, ungauged tributaries are a
23 | significant contributor to this increase and can be a contributor even during low flow periods.

24 | 4 Discussion

25 | 4.1 Baseflow estimates

26 | Digital baseflow filters separate out the 'slow flow' component of streamflow. As such, they
27 | provide an effective upper bound on possible groundwater discharge to streamflow
28 | (Cartwright et al., 2014). This was tested by plotting [scatter plots of](#) baseflow estimates for
29 | the Gellibrand River from [Eckhardt](#) digital filter [analysis, residual streamflow \(i.e. Bunker](#)
30 | [Hill discharge less other gauged tributaries lagged by one day – Upper Gellibrand, Lardner](#)
31 | [Creek, Love Creek\)](#) and tracer mass balance analyses (Fig. 109 a, b, c) for the 2011-2013
32 | period. The tracer estimates include the range of estimates from Atkinson et al. (2014, 2015)

1 for sampling from known dates conducted in 2011-2012 using ^{222}Rn and Cl mass balance,
2 plus the results from this study for sampling in 2013 using major ions (shown as mid-points of
3 the range for each date shown in Table 1). None of these estimates are directly comparable as
4 they measure different components of baseflow but their comparison is informative. The
5 digital filter time-series estimates baseflow from the entire catchment upstream of Bunker Hill
6 gauging station. The Atkinson et al. (~~2014~~2015) estimates are for the groundwater discharge
7 component of streamflow measured over the alluvial valley reach (approximately two thirds
8 of the Bunker Hill to Upper Gellibrand reach, see Fig. 1) and use a two end-member mass
9 balance approach (tributary inflow was not considered). The tracer mass balance results from
10 our study are for the groundwater discharge component of baseflow over the Bunker Hill to
11 Upper Gellibrand reach and account for ungauged tributary inflow. For additional
12 comparison, the ~~10-day average~~ residual monthly discharge, monthly baseflow (~~i.e. Bunker~~
13 ~~Hill discharge less other gauged tributaries lagged by one day~~ ~~Upper Gellibrand, Lardner~~
14 ~~Creek, Love Creek~~) and the ~~mean-daily~~ monthly saturated volume change for months with
15 decreasing volumes were ~~analysed-plotted~~ (Sect. 3.4, Fig. 9ed). The saturated volume change
16 was calculated with a realistic specific yield range (set 0.15, 0.3, 0.05 in Table 2) that
17 produces a relatively high estimate of groundwater discharge compared to estimates using
18 other specific yield values (see Table 2).

19 The tracer estimates of groundwater discharge and the residual discharge ~~vary considerably~~
20 ~~around the digital filter baseflow time-series~~ generally show a consistent relationship (Fig.
21 ~~109a~~). The Atkinson et al. (2015) estimates coincided with the residual discharge, except for
22 two outliers from one date sampled on a small rising limb, but neither methods separates out
23 in-reach tributary flow from groundwater discharge. The tracer estimates from this study used
24 the residual discharge as an upper bound in their estimation and so show a high correlation
25 and a negative bias with the residual discharge. When the tracer estimates ~~are~~ plotted against
26 ~~the two~~ baseflow filter estimates (Fig. 9b, using $a=0.988$, $\text{BFI}_{\text{max}}=0.2$ and $a=0.988$,
27 $\text{BFI}_{\text{max}}=0.6$) the relationships are poorly correlated and with the tracer estimates both under-
28 and over-estimating relative to the baseflow filter estimates. ~~In particular, the residual~~
29 ~~discharge is larger than the digital filter baseflow during high flow periods but can be lower~~
30 ~~during low flow periods.~~ The use of ~~a~~ the larger BFI_{max} value (0.6), more consistent with the
31 recommendations of Eckhardt (2005), ~~would increase the digital filter estimates but would~~
32 ~~also result in more periods of baseflow greater than total streamflow~~ results in the tracer
33 estimates having a more consistently being underestimated negative bias relative to the

1 baseflow filter estimates. The daily residual discharge is also compared to the baseflow filter
2 estimates over the period 2007-2013 (Fig. 9c). The use of the larger BFI_{max} value results in
3 baseflow generally higher than the residual flow (but with considerable scatter) while the
4 lower BFI_{max} value results in baseflow generally lower than the residual discharge,
5 particularly at high discharges. Finally, the mapped monthly changes in saturated
6 groundwater volume (see Fig. 87) were plotted against the monthly residual discharge and
7 baseflow filter estimates (using $a=0.988$, $BFI_{max}=0.2$ and 0.6) over the 2007-2010 period (Fig.
8 9d). The saturated volume changes were typically lower than both the residual discharge and
9 the two baseflow discharges, consistent with the latter two the residual and baseflow measures
10 providing an upper bound to groundwater discharge within the study reach. Even the estimate
11 of groundwater volume change (is more likely to be considered as represent an upper bound
12 estimate than an unbiased estimate due to the use of a relatively high specific yield range and
13 not accounting for phreatic evapotranspiration) generally sits below the baseflow and residual
14 discharge estimates.

15 Tracer data can also be used to calibrate the BFI_{max} parameter in the Eckhardt digital filter
16 (Gonzalez et al., 2009) if a suitable end-member signature can be identified. However, in
17 catchments with low salinity alluvial groundwater (i.e. catchments with low groundwater
18 residence time), end-member differentiation can be an issue (Kendall et al., 2001). ~~For~~
19 ~~example, the Atkinson et al. (2014) mass balance estimates of groundwater discharge~~
20 ~~generally cluster around the residual discharge time series but neither separate out in reach~~
21 ~~tributary flow from groundwater discharge. This could be an important distinction for water~~
22 ~~resource management.~~

23 The different estimates of baseflow and groundwater discharge emphasise the difficulties in
24 separating and defining these important fluxes, particularly how they vary seasonally. In the
25 context of the catchment used in this study, these variations raise questions of whether the in-
26 reach tributary inflow can be lumped with groundwater discharge (i.e. does regional
27 groundwater discharge also drive tributary flow) and does the digital baseflow filter analysis
28 overestimate groundwater discharge during high flow periods. This separation of
29 groundwater discharge from other slow flow pathways (e.g. interflow or perched aquifer
30 discharge driving tributary flow) could be an important distinction for water resource
31 management.

4.2 Baseflow—water table dynamics and uncertainties

The first two hypotheses addressed by this paper involve the ability of monthly water table/groundwater surface dynamics to explain monthly variations in digital filter estimated baseflow. Large increases in baseflow during the high flow season (e.g. winter-spring) could also contain contributions from other slow fluxes (e.g. interflow and perched aquifer discharge contributing to tributary flow, bank storage return). In order to avoid overestimations of groundwater discharge, it is important to independently test the assumption of a single storage (i.e. regional groundwater) driving baseflow.

In terms of the groundwater contribution, we postulated that the main driver of large increases in baseflow would be non-linear increases in the discharge area as groundwater levels rose and intersected more of the land surface. Monthly water table/groundwater surfaces were used to test whether such increases in discharge area are a feasible mechanism. In the case of the Gellibrand catchment, the water table/groundwater data showed that only modest increases in possible discharge area occurred during the seasonal peaks in groundwater levels. and the The pattern in the magnitude of seasonal peaks of digital filter estimated baseflow was similar to that shown by the water table surfaces but not by the potentiometric surfaces.~~in this measure showed a poor coincidence with the magnitude of seasonal peaks of digital filter estimated baseflow.~~ The limited seasonal variations in the potentiometric surfaces probably reflect the upward gradients observed in bores screened in the Eastern View Formation. The mapped water table surfaces rarely reach the ground surface but the large seasonal variations in the water table within 1 m of the ground surface (Fig. 6b) are likely to interact with the drainage system along the valley, particularly within the uncertainty range of the groundwater mapping. ~~Uncertainties in the geostatistically defined groundwater surfaces were not considered to significantly affect the relationship between discharge area and estimated baseflow. Most monitoring bores were located in the valley floors and so confidence in the interpolated water table surfaces was highest in these areas. Consequently, varying the definition of discharge area (i.e. from 0 to 1 m below the ground surface) did not result in large changes (Fig. 7a). However, fluctuations~~ Fluctuations in the water table remain a relatively coarse measure and provide only a first-order estimate of possible groundwater discharge patterns. For instance, the mapping ~~may does~~ not have the resolution to identify the fine detail of channels and near-stream zones. Stage variations in channels will have local effects on groundwater recharge and discharge that are not captured by the groundwater

1 mapping. Likewise, where capillary fringing effects in near-stream zones could lead to large
2 increases in discharge rapid increases in the water table with a small rise in water content in
3 the unsaturated zone (Gillham, 1984). Furthermore, the spatial correlation (as defined by the
4 model variogram) may vary with the groundwater level (Lyon et al. 2006, Peterson et al,
5 2011) and alternative external drift terms to land surface elevation, such as topographic
6 wetness index, could possibly better represent near-stream spatial heterogeneity.

7 The water table groundwater mapping technique also assumes that the groundwater – river
8 interaction is dominated by unconfined groundwater. Atkinson et al. (~~2014~~2015) found that
9 much of the estimated groundwater discharge (50-90%) in the study catchment was occurring
10 over a short 5-10 km reach where the river intersected outcropping Eastern View Formation,
11 the main regional semi-confined aquifer. It is quite possible that variations in discharge from
12 this regional aquifer may not be adequately represented by changes in the unconfined
13 potentiometric groundwater surfaces or the water table. However, temporal changes in the
14 saturated volume of the unconfined groundwater, as estimated by water table groundwater
15 surface mapping, should provide a first order control on the total amount of groundwater
16 discharge. The digital filter estimates of baseflow were generally significantly larger in the
17 spring early summer period most months than could be explained by generous estimates of
18 groundwater volume change in these periods using specific yield values likely to represent the
19 upper bound of the specific yield range of the different geological units within the catchment.
20 This ‘excess’ baseflow most likely represents interflow and hillslope perched aquifer
21 discharge contributing to streamflow as the catchment drains following the winter-spring wet
22 season.

23 The generation of the potentiometric surface (using 988 bores) and the water table (using 33
24 bores) gives an indication of the sensitivity of the use of groundwater surface mapping to the
25 amount of data available. The maps generated from the two datasets showed some
26 differences, particularly in the minimum depths to groundwater and the increase in the
27 standard deviation of the water table dataset (e.g. see Fig. 5). The increase in the standard
28 deviation of each monthly groundwater surface from the use of fewer bores demonstrates the
29 expected result that confidence in the groundwater mapping analysis will decrease with fewer
30 data points. However, in the case of the Gellibrand catchment, the similar estimates of
31 monthly saturated volume changes from both datasets (Fig. 8) indicated that the relative
32 differences between monthly groundwater surfaces generated by the two datasets were small.

1 Uncertainties in the geostatistically defined groundwater surfaces were not considered to
2 significantly affect the relationship between discharge area and estimated baseflow. This is
3 probably reflects that because Most monitoring bores in both datasets were located in the
4 valley floors and so confidence in the interpolated water table surfaces was highest in these
5 areas. which These areas are also of most interest in investigating groundwater – river
6 interactions. The effectiveness of groundwater mapping as a water resource assessment tool
7 will be determined by depend on the amount number of monitoring bores within a catchment-
8 but The the question of how many monitoring bores are required will be highly dependent on
9 the catchment size and spatial distribution of bores. In this study area, monitoring bores were
10 commonly located in clusters and transects of limited length and these locations were likely
11 determined by ease of access for drilling and the specific aims of past investigations rather
12 than to optimise the spatial distribution of groundwater observations for catchment wide water
13 table mapping. As a result, the uncertainty of groundwater surface maps would be very
14 catchment specific and difficult to generalise to other locations.

15 **4.3 End member – water table dynamics**

16 The geostatistical mapping of groundwater surfaces in conjunction with terrain analysis
17 allows the testing of end-member assumptions. For example, streamflow from small
18 tributaries during dry periods could be sourced primarily from regional unconfined
19 groundwater or perched aquifer – interflow type processes. Given the lack of availability of
20 piezometers targeting the latter pathways in most catchments, the capacity to test the possible
21 source of tributary flow provides important information on the suitability of the tributary flow
22 as a separate end-member to flow in the main river. In this context, the results from this study
23 clearly show that much of the small tributary flow in the Gellibrand catchment has a similar
24 chemical signature to the regional groundwater. Nevertheless, most tributaries were sampled
25 from sub-catchments with regional groundwater significantly deeper than the land surface.
26 The chemical similarities between the small tributary flow (probably representing interflow)
27 and the regional groundwater was not unexpected given that it is likely that this interflow
28 development is the major contributor to the deeper regional groundwater recharge. The ionic
29 similarities between these end-members illustrate that mass balance techniques will struggle
30 to separate these fluxes with any confidence and that additional, independent data, such as
31 water table mapping, are required to confidently identify the groundwater discharge flux.

1 **5 Conclusions**

2 Geostatistical mapping of unconfined groundwater surfaces provides a useful, independent
3 dataset for investigating sources of fluxes contributing to baseflow estimated by traditional
4 digital filter and tracer end-member approaches. In particular, the method can provide added
5 confidence in the lower bound of baseflow estimates that best correspond to regional
6 groundwater discharge in both low and high flow periods. Specifically, the groundwater
7 surface dataset can be used to identify whether variations in discharge area (i.e. groundwater
8 intersecting the land surface) or saturated volume can explain seasonal variations in baseflow,
9 as estimated using digital filters. This dataset is particularly useful in humid, hilly catchments
10 where interflow or perched aquifer discharge is likely to be a significant process and where
11 the different ‘slow flow’ fluxes have similar low salinity chemistry ~~and relatively short~~
12 ~~residence times that hinders end-member analysis.~~ Sufficient monitoring bore data to construct
13 water table maps are not available in all catchments and the method is likely to be restricted to
14 catchments where groundwater investigations have resulted in the existence of an adequate
15 bore network. The adequacy of the network will depend on catchment size, the spatial
16 distribution of bores (i.e. uniform versus non-uniform distribution, location relative to the
17 drainage network) and the spatial correlation of the monitored water level. However, where
18 adequate monitoring data are available, this method adds significant value to water resource
19 management by making better use of an independent, but often under-utilised, dataset that can
20 inform groundwater contributions to streamflow.~~Sufficient monitoring bore data to construct~~
21 ~~water table maps are not available in all catchments but this method adds significant value to~~
22 ~~water resource management where these monitoring data are available.~~

23 **Author contributions**

24 J. C., A. W. and J. M. designed the field experiments and analyses. K. H and T. P. designed
25 and carried out the [water table groundwater](#) mapping with T. P. developing the model code for
26 the temporal interpolation of groundwater observations and mapping of groundwater surfaces.
27 J. C. carried out most of the data analysis and prepared the manuscript with contributions
28 from all co-authors.

29 **Acknowledgements**

30 This work is funded by the Australian Research Council Discovery Project scheme through
31 project DP120100253. We greatly appreciate the provision of groundwater chemistry data and
32 introduction to the Gellibrand catchment by Dr Alex Atkinson and Professor Ian Cartwright

1 from Monash University. [We thank two anonymous reviewers and Professor Ian Cartwright](#)
2 [for their insightful and constructive reviews that helped improve this paper.](#)

4 **References**

5 [Abedini, M. J., Nasser, M., and Burn, D. H.: The use of a genetic algorithm-based search](#)
6 [strategy in geostatistics: application to a set of anisotropic piezometric head data,](#)
7 [Comput. Geosci., 41, 136-146, 2012.](#)

8 [Atkinson, A. P., Cartwright, I., Gilfedder, B. S., Cendón, D. I., Unland, N. P., and Hofmann,](#)
9 [H.: Using 14C and 3H to understand groundwater flow and recharge in an aquifer](#)
10 [window, Hydrol. Earth Syst. Sci., 18, 4951–4964, 2014.](#)

11 Atkinson, A. P., Cartwright, I., Gilfedder, B. S., Hofmann, H., Unland, N. P., Cendón, D. I.,
12 and Chisari, R.: A multi-tracer approach to quantifying groundwater inflows to an upland
13 river; assessing the influence of variable groundwater chemistry, Hydrol. Process., [29, 1-](#)
14 [12](#), 10.1002/hyp.10122, 2014⁵.

15 Boezio, M. N. M., Costa, J. F. C. L. & Koppe, J. C.: Kriging with an external drift versus
16 collocated cokriging for water table mapping, Applied Earth Science: Transactions of the
17 Institution of Mining & Metallurgy, Section B, 115, 103-112, 2006.

18 [Bredehoeft, J. D., Papadopoulos, S. S., and Cooper, H. H. Jr.: Groundwater: the water budget](#)
19 [myth in scientific basis of water resource management. National Research Council](#)
20 [Geophysics Study Committee, National Academy Press, Washington, DC, pp 51–57,](#)
21 [1982.](#)

22 [Brutsaert, W.: Long-term groundwater storage trends estimated from streamflow records:](#)
23 [Climatic perspective, Water Resour. Res., 44, W02409, doi:10.1029/2007WR006518,](#)
24 [2008.](#)

25 Cartwright, I., Hofman, H., Sirianos, M. A., Weaver, T. R., and Simmons, C. T.: Geochemical
26 and ²²²Rn constraints on baseflow to the Murray River, Australia, and timescales for the
27 decay of low-salinity groundwater lenses, J. Hydrol., 405, 333-343, 2011.

28 Cartwright, I., Gilfedder, B., and Hofmann, H.: Contrasts between chemical and physical
29 estimates of baseflow help discern multiple sources of water contributing to rivers,
30 Hydrol. Earth Syst. Sci., 18, 15–30, 2014.

- 1 Chen, X. and Wang, D.: Evaluating the effect of partial contributing storage on the storage –
2 discharge function from recession analysis, *Hydrol. Earth Syst. Sci.* 17, 4283–4296,
3 2013.
- 4 Cook, P. G., Favreau G., Dighton J. C., and Tickell S.: Determining natural groundwater
5 influx to a tropical river using radon, chlorofluorocarbons and ionic environmental tracers,
6 *J. Hydrol.*, 277, 74-88, 2003.
- 7 Desbarats, A. J., Logan, C. E., Hinton, M., and Sharpe, D. R.: On the kriging of water table
8 elevations using collateral information from a digital elevation model, *J. Hydrol.*, 255 (1-
9 4), 25–38, 2002.
- 10 Eckhardt, K.: How to construct recursive digital filters for baseflow separation, *Hydrol.*
11 *Process.*, 19, 507-515, 2005.
- 12 Eckhardt, K.: A comparison of baseflow indices, which were calculated with seven different
13 baseflow separation methods, *J. Hydrol.*, 352, 168-173, 2008.
- 14 Fenicia, F., Savenije, H. H. G., Matgen, P., and Pfister, L.: Is the groundwater reservoir linear?
15 Learning from data in hydrological modelling, *Hydrol. Earth Syst. Sci.*, 10, 139-150, 2006.
- 16 Gillham, R. W.: The capillary fringe and its effect on water-table response. *J. Hydrol.*, 67, 307-
17 324, 1984.
- 18 Gonzales, A. L., Nonner, J., Heijkers, J., and Uhlenbrook, S.: Comparison of different base
19 flow separation methods in a lowland catchment, *Hydrol. Earth Syst. Sci.*, 13, 2055-2068,
20 2009.
- 21 Jencso, K. G. and McGlynn, B.L.: Hierarchical controls on runoff generation: Topographically
22 driven hydrologic connectivity, geology and vegetation, *Wat. Resour. Res.*, 47, W11527,
23 doi:10.1029/2011WR010666, 2011.
- 24 Jencso, K. G., McGlynn, B. L., Gooseff, M. N., Wondzell, S. M., Bencala, K. E., and
25 Marshall, L. A.: Hydrologic connectivity between landscapes and streams: Transferring
26 reach- and plot-scale understanding to the catchment scale, *Water Resour. Res.*, 45,
27 W04428, doi:10.1029/2008WR007225, 2009.
- 28 ~~Jones, J. P., Sudicky, E. A., Brookfield, A. E., Park, Y-J.: An assessment of the tracer based~~
29 ~~approach to quantifying groundwater contributions to streamflow, *Water Resour. Res.*, 42,~~
30 ~~W02407, 2006.~~

- 1 Kendall, C., McDonnell, J. J., and Gu, W.: A look inside ‘black box’ hydrograph separation
2 models: a study at the Hydrohill catchment, *Hydrol. Process.*, 15, 1877-1902, 2001.
- 3 Leblanc, M., Tweed, S., Van Dijk, A., and Timbal, B.: A review of historic and future
4 hydrological changes in the Murray-Darling Basin, *Glob. Planet. Change*, 80-81, 226-246,
5 2012.
- 6 [Li, L., Maier, H. R., Partington, D., Lambert, M. F. and Simmons, C. T.: Performance](#)
7 [assessment and improvement of recursive digital baseflow filters for catchments with](#)
8 [different physical characteristics and hydrological inputs, *Environ. Modell. Softw.*, 54, 39-](#)
9 [52, 2014.](#)
- 10 Llamas, M. R. and Martínez-Santos, P.: Intensive groundwater use: Silent revolution and
11 potential source of social conflicts, *J. Water Res. Plan. Manag.*, 131, 337-341, 2005.
- 12 [Love, A. J., Herczeg, A. L., Armstrong, D., Stadter, F., and Mazor, E.: Groundwater flow](#)
13 [regime within the Gambier Embayment of the Otway Basin, Australia: evidence from](#)
14 [hydraulics and hydrochemistry, *J. Hydrol.*, 143, 297–338, 1993.](#)
- 15 Lyon, S. W., Seibert, J., Lembo, A. J., Walter, M. T. and Steenhuis, T. S. : Geostatistical
16 investigation into the temporal evolution of spatial structure in a shallow water table,
17 *Hydrol. Earth Syst. Sci.*, 10, 113-125, 2006.
- 18 [McCallum, J. L., Cook, P. G., Brunner, P. and Berhane, D.: Solute dynamics during bank](#)
19 [storage flows and implications for chemical base flow separation. *Wat. Resour. Res.*, 46,](#)
20 [W07541, doi:10.29/2009WR008539, 2010.](#)
- 21 McGlynn, B. L. and McDonnell, J. J.: Quantifying the relative contribution of riparian and
22 hillslope zones to catchment runoff, *Wat. Resour. Res.*, 39 (11), 1310,
23 doi:10.1029/2003WR002091, 2003.
- 24 Meshgi, A., Schmitter, P., Babovic, V. and Chui, T. F. M.: An empirical method for
25 approximating stream baseflow time series using groundwater table fluctuations, *J.*
26 *Hydrol.*, 519, 1031-1041, doi: 10.1016/j.jhydrol.2014.08.033, 2014.
- 27 Nathan, R. J. and McMahon, T. A.: Evaluation of automated techniques for base flow and
28 recession analyses, *Wat. Resour. Res.*, 26 (7),1465-1473, 1990.
- 29 Nwankwor, G. I., Cherry, J. A., and Gillham, R. W.: A comparative study of specific yield
30 determinations for a shallow sand aquifer, *Ground Water*, 22, 764-772, 1984.

- 1 [Ortiz, C. J. and Deutsch, C. V.: Calculation of uncertainty in the variogram, *Math. Geol.*, 34,](#)
2 [169-18, 2002.](#)
- 3 Perrin, J., Mascré, C., Pauwels, H., Ahmed, S.: Solute recycling: An emerging threat to
4 groundwater quality in southern India, *J. Hydrol.*, 398, 144-154, 2011.
- 5 Peterson, T. J. and Western, A. W.: Nonlinear time-series modeling of unconfined groundwater
6 head, *Wat. Resour. Res.*, [50, 8330-8355](#), doi: 10.1002/2013WR014800, [in-press2014](#).
- 7 Peterson, T. J., Cheng, X., Western, A. W., Siriwardena, L., and Wealands, S. R.: Novel
8 indicator geostatistics for water table mapping that incorporate elevation, land use, stream
9 network and physical constraints to provide probabilistic estimation of heads and fluxes,
10 in: Proceeding of the 19th International Congress on Modelling and Simulation, Perth,
11 Australia, 12–16 December 2011, 3910-3916, 2011.
- 12 SKM, (2012), Newlingrook groundwater investigation – Gellibrand River streambed and
13 baseflow assessment, Report to Barwon Water, Geelong, Australia, available at:
14 <http://www.barwonwater.vic.gov.au/vdl/A5711327/Newlingrook> groundwater
15 investigation - Gellibrand River streambed and baseflow assessment (report by SKM
16 consultants).pdf., [last access: 21 January 2014](#), 2012.
- 17 [SKM, \(2010\), Glenelg Hopkins CMA groundwater model – final model development report,](#)
18 [Report to the Victorian Department of Sustainability and Environment, available at:](#)
19 https://ensym.dse.vic.gov.au/docs/GlenelgHopkins_TransientModelReport_FINAL.pdf,
20 [last access: 5 February 2015, 2010.](#)
- 21 [Sophocleous, M.: From safe yield to sustainable development of water resources – the Kansas](#)
22 [experience, *J. Hydrol.*, 235, 27-43, 2000.](#)
- 23 [Sophocleous, M.: Interactions between groundwater and surface water; the state of the science,](#)
24 [Hydrogeol. J., 10 \(2\), 52-67, 2002.](#)
- 25 Tallaksen, L. M.: A review of baseflow recession analysis, *J. Hydrol.*, 165, 349-370, 1995.
- 26 van Dijk, A. I., Beck, H. E., Crosbie, R. S., de Jeu, R. A., Liu, Y. Y., Podger, G. M., Timbal,
27 B., and Viney, N. R.: The Millennium Drought in southeast Australia (2001-2009):
28 Natural and human causes and implications for water resources, ecosystems, economy,
29 and society, *Wat. Resour. Res.*, 49, 1040-1057, doi:10.1002/wrcr.20123, 2013.

- 1 Ward, R. C. and Robinson, M.: Principles of Hydrology, 4th edn., McGraw-Hill, New York,
2 2000.
- 3 Wittenberg, H., and Sivapalan, M.: Watershed groundwater balance estimation using stream-
4 flow recession analysis and baseflow separation, Hydrol. Process., 13, 715-726, 1999.
- 5 Wittenberg, H.: Baseflow recession and recharge as nonlinear storage processes, J. Hydrol.,
6 219, 20-33, 1999.
- 7 Woessner, W. W.: Stream and fluvial plain ground water interactions: rescaling
8 hydrogeologic thought, Ground Water, 38 (3), 423-429, doi: 10.1111/j.1745-
9 6584.2000.tb00228.x, 2000.
- 10

1 Table 1. Estimates of groundwater discharge (Q_{gw}) and ungauged tributary discharge (Q_{ut})
2 using mass balance analysis and mean measured compositions of groundwater and ungauged
3 tributary flow. The values within the brackets are the range of valid discharges generated by
4 varying the groundwater composition by one standard deviation for each ion used in the
5 analysis. Q_{res} is the residual discharge after accounting for the gauged discharges within the
6 study catchment and the following value in brackets is the ratio of Q_{res} to the total streamflow
7 measured at Bunker Hill gauging station. *solution poorly constrained.

Date	Q_{gw} (MLd ⁻¹)	Q_{ut} (MLd ⁻¹)	Q_{res} (MLd ⁻¹)	Tracer	Method
21/1/13	14.0 (4.0-14.0)	2.8 (2.8-12.8)	16.8 (0.45)	Cl-Ca	Two end-member
21/1/13	12.0 (7.0-12.0)	4.8 (4.8-9.8)	16.8 (0.45)	Cl-Mg	Two end-member
21/1/13	14.8 (1.3-14.8)	2.0 (2.0-15.5)	16.8 (0.45)	Ca-Mg	Two end-member
21/1/13	- (4.4-7.6)	- (9.2-12.4)	16.8 (0.45)	Na-Mg	Two end-member
21/1/13	- (10.3)	- (6.5)	16.8 (0.45)	Na-Ca	Two end-member
21/1/13 – 28/1/13	13.7 (5.3-13.7)	1.8 (1.8-10.2)	15.5 (0.45)	Cl	One end-member series
21/1/13 – 28/1/13	7.1 (3.8-12.6)	8.4 (2.9-11.7)	15.5 (0.45)	Na	One end-member series
21/1/13 – 28/1/13	13.7 (8.9-13.7)	1.8 (1.8-6.6)	15.5 (0.45)	Ca	One end-member series
21/1/13 – 28/1/13	13.7 (7.7-13.7)	1.8 (1.8-7.9)	15.5 (0.45)	Mg	One end-member series
21/1/13 – 28/1/13	4.7 (3.3-8.2)	10.8 (7.3-12.2)	15.5 (0.45)	¹⁸ O	One end-member series
21/1/13 – 28/1/13	8.1 (4.6-8.1)	7.5 (7.5-10.9)	15.5 (0.45)	² H	One end-member series
7/6/13	25.2 (20.5-25.4)	59.6 (59.4-64.3)	84.8 (0.43)	Cl-Na	Two end-member
7/6/13	48.8 (35.6-53.2)	36.0 (31.6-49.2)	84.8 (0.43)	Na-Mg	Two end-member
7/6/13	38.2 (7.5-38.2)	46.6 (46.6-77.3)	84.8 (0.43)	Cl-Ca	Two end-member
7/6/13	68.9 (36.6-68.9)	15.9 (15.9-48.2)	84.8 (0.43)	Cl-Mg	Two end-member
7/6/13	9.8 (9.8-16.6)	75.0 (68.2-75.0)	84.8 (0.43)	Na-Ca	Two end-member
7/6/13 - 11/6/13	- (18.8-29.9)	- (17.1-28.2)	47.0 (0.41)	Cl	One end-member series
7/6/13 - 11/6/13	2.2 (1.2-20.5)	44.8 (26.5-45.8)	47.0 (0.41)	Na	One end-member series
20/6/13	14.7 (10.0-14.9)	31.0 (30.8-35.7)	45.7 (0.38)	Cl-Na	Two end-member
20/6/13	42.4 (3.8-42.4)	3.3 (3.3-34.3)	45.7 (0.38)	Na-Mg	Two end-member
20/6/13	- (44.5)	- (1.2)	45.7 (0.38)	Cl-Mg	Two end-member
20/6/13	- (0.2-1.0)	- (34.8-35.6)	45.7 (0.38)	Cl-Ca	Two end-member
20/6/13	- (15.3-17.9)	- (17.9-20.5)	45.7 (0.38)	Na-Ca	Two end-member
18/6/13 - 20/6/13	51.9 (31.3-51.9)	0.3 (0.3-20.9)	52.2 (0.42)	Cl	One end-member series
18/6/13 - 20/6/13	- (27.3-36.4)	- (15.8-24.9)	52.2 (0.42)	Na	One end-member series
18/6/13 - 20/6/13	0.0- (36.9)	- 52.2(15.3)	52.2 (0.42)	Cl-Na	Two end-member series*
18/6/13 - 20/6/13	51.9- (17.3-45.2)	0.3- (7.0-34.9)	52.2 (0.42)	Ca-Mg	Two end-member series*
16/12/13	5.3 (5.3-26.6)	30.6 (9.2-30.6)	35.8 (0.30)	Na-Ca	Two end-member
16/12/13	17.1 (0.2-17.1)	18.7 (18.7-35.8)	35.8 (0.30)	Cl-Ca	Two end-member
16/12/13	- (16.2-16.6)	- (19.2-19.6)	35.8 (0.30)	Na-Cl	Two end-member
16/12/13	- (3.8-12.6)	- (23.2-32.1)	35.8 (0.30)	Na-Mg	Two end-member
16/12/13	- (18.0)	- (17.8)	35.8 (0.30)	Ca-Mg	Two end-member
16/12/13	- (2.3-33.4)	- (2.4-33.6)	35.8 (0.30)	Cl-Mg	Two end-member

8
9

1 Table 2. Minimum, median and 90th percentile values for ratio of monthly Eckhardt filter
 2 baseflow to ‘water table’ volume changes using a range of specific yields (S_{y1} - Wangerrip
 3 Group, S_{y2} – alluvium, S_{y3} – Heytesbury Group aquitards). Filtered baseflow time-series were
 4 calculated using a value of 0.988 and BFI_{max} values of 0.2 or 0.6. Only months with declining
 5 volume changes were used in the analysis.

<u>S_{y1}, S_{y2}, S_{y3}</u>	<u>Min ratio</u>		<u>Median ratio</u>		<u>90th perc. ratio</u>	
	<u>$BFI_{max} = 0.2$</u>	<u>0.6</u>	<u>0.2</u>	<u>0.6</u>	<u>0.2</u>	<u>0.6</u>
<u>0.1, 0.3, 0.05</u>	<u>0.41</u>	<u>0.89</u>	<u>3.23</u>	<u>10.81</u>	<u>27.3</u>	<u>57.3</u>
<u>0.1, 0.2, 0.05</u>	<u>0.41</u>	<u>0.89</u>	<u>3.88</u>	<u>12.89</u>	<u>28.4</u>	<u>61.7</u>
<u>0.1, 0.1, 0.05</u>	<u>0.41</u>	<u>0.89</u>	<u>6.77</u>	<u>18.06</u>	<u>38.0</u>	<u>80.2</u>
<u>0.15, 0.3, 0.05</u>	<u>0.27</u>	<u>0.59</u>	<u>2.52</u>	<u>8.59</u>	<u>15.9</u>	<u>33.9</u>
<u>0.05, 0.05, 0.05</u>	<u>0.82</u>	<u>1.78</u>	<u>11.9</u>	<u>32.21</u>	<u>49.8</u>	<u>12.5</u>
<u>0.1, 0.1, 0.1</u>	<u>0.41</u>	<u>0.89</u>	<u>5.96</u>	<u>16.11</u>	<u>24.9</u>	<u>60.2</u>
<u>0.2, 0.2, 0.2</u>	<u>0.21</u>	<u>0.45</u>	<u>2.98</u>	<u>8.05</u>	<u>12.4</u>	<u>30.1</u>
<u>0.3, 0.3, 0.3</u>	<u>0.14</u>	<u>0.30</u>	<u>1.99</u>	<u>5.37</u>	<u>8.3</u>	<u>20.1</u>

6
7

1 Figure 1. Location and geology of Gellibrand River catchment in Victoria, Australia showing
2 catchment and gauged subcatchment boundaries, monitoring bores, gauging stations and
3 Sayers Bridge (ungauged) river sampling location.

4

5 Figure 2. Hydrograph at Bunker Hill gauging station (235227) illustrating the seasonality of
6 flow. ~~The 30th, 40th and 50th percentiles of flow based on the entire record (1979–2013) are~~
7 ~~shown along with periods of streamflow hydrochemical sampling.~~ Three baseflow separation
8 hydrographs generated using different BFI_{max} parameter values (0.20, 0.60, 0.80 and $a=0.988$)
9 for the Eckhardt filter are displayed, along with the periods of hydrochemical sampling of
10 streamflow during 2013.

11

12 Figure 3. Piper diagrams showing temporal and spatial patterns in the chemistry of
13 streamflow and groundwater. The top panel shows seasonal variations in composition of flow
14 in the Gellibrand River at the upstream (Upper Gellibrand) and downstream (Bunker Hill)
15 sites over three sampling trips. The internal arrows show direction of compositional change
16 from upstream to downstream and also from summer to winter towards the general
17 groundwater composition. The lower panel shows compositional differences across all
18 sampling trips between Gellibrand River, gauged tributaries, ungauged tributaries and
19 groundwater.

20

21 ~~Figure 4. Stable isotope data for streamflow and groundwater samples from three sampling~~
22 ~~trips (January, June and December 2013). The local Meteoric Water Line (LMWL) for~~
23 ~~Melbourne is shown for comparison (IAEA/WMO 2006 Global Network of Isotopes in~~
24 ~~Precipitation data).~~

25

26 Figure 54. ~~Stable isotope and major~~ Major ion changes during streamflow recession of
27 January 2013 measured at Bunker Hill gauging station. Concentrations are divided by the
28 mean concentration of the sampling period for each tracer.

29

1 Figure 65. Depth to ~~water table~~groundwater maps (A – ‘potentiometric surface’ (all bores), B
2 –‘water table’ (shallow bores)) and kriging standard deviation (~~BC – potentiometric surface,~~
3 D – water table) for 1st September 2009. Areas of shallow or intersecting (artesian) ~~water~~
4 tablegroundwater are restricted to the Gellibrand River (centre) and Love Creek (north) valley
5 floors.~~The variations in artesian water table areas between shallower (September) and deeper~~
6 ~~(March) water tables are relatively minor.~~

7
8 Figure 76. ~~(a)~~Percentage saturated area (intersection of groundwater surface with land
9 surface) variations over time for the potentiometric (all bores) dataset (a) and the water table
10 (33 bores) dataset (b) for the catchment area with elevation <100 m. The position of the water
11 table is shown for ~~five~~three depths (0, 0.5, –1.0 m) to allow for uncertainties in the mapping
12 of the depth to water table. ~~(b) Variations in percentage saturated area against~~The mean daily
13 ~~monthly~~ baseflow for each month is shown for two sets of Eckhardt filter parameter values
14 calculated from the ~~three time series generated using the Eckhardt baseflow filter for the~~
15 Bunker Hill gauging record. Baseflow 1 uses the low BFI_{max} value ($a=0.988$, $BFI_{max}=0.20$)
16 while Baseflow 2 uses a higher BFI_{max} value ($a=0.988$, $BFI_{max}=0.60$).

17
18 Figure 87. Monthly variations in saturated volumes for the catchment area with elevation
19 <100 m for both the potentiometric and water table datasets and for monthly baseflow derived
20 from Eckhardt analysis (using BFI_{max} value of 0.2).

21
22 Figure 98. Piper diagram (right) shows tributary samples grouped by the minimum depth to
23 groundwater table in the sub-catchment upstream of the sampling point. Compositions of
24 sampled groundwater bores are also shown. The spatial location and sub-catchment extent are
25 shown superimposed on the potentiometric ~~depth of water table~~to groundwater map for
26 September 2010.

27
28 Figure 9. Scatter plots showing various estimates of baseflow and groundwater discharge. (a)
29 Mass balance tracer estimates (from Atkinson et al. (2015) for 2011-2012 and mid-point of
30 range shown in Table 1 for 2013) for groundwater discharge against the residual streamflow
31 (Bunker Hill streamflow less upstream gauged streamflow). (b) Mass balance tracer estimates

1 ~~against the Eckhardt filter baseflow estimates (Qb1 uses $a=0.988$ and $BFI_{max}=0.2$, Qb2 uses~~
2 ~~$a=0.988$ and $BFI_{max}=0.6$). (c) Residual discharge against Eckhardt filter baseflow timeseries~~
3 ~~for 2007-2013. (d) Saturated volume changes (using specific yield set 0.15, 0.30, 0.05 from~~
4 ~~Table 2) against residual flow and Eckhardt filter baseflow timeseries.~~Figure 109.
5 ~~Hydrograph at Bunker Hill gauging station (235227) showing various estimates of baseflow~~
6 ~~and groundwater discharge. The Bunker Hill discharge and mean estimate of baseflow using~~
7 ~~three sets of parameter values for the Eckhardt filter are as shown in Fig. 2. Also shown is the~~
8 ~~10 day mean residual discharge at Bunker Hill (Qdiff) after accounting for all gauged~~
9 ~~tributary inflow (lagged by one day) and the mean monthly saturated volume change (as~~
10 ~~shown in Figure 8). The midpoint and range of estimates of groundwater discharge from~~
11 ~~tracer analysis are shown for 2011-2012 (Atkinson et al., 20142015) and 2013 (this study).~~
12